PREDIS

# Deliverable 4.3
# Development of vacuumable gels for the decontamination of metallic surfaces

Date 29.2.2024 version Final

Public

Alban Gossard
CEA Marcoule
30207 Bagnols-sur-Cèze
FRANCE

alban.gossard@cea.fr
+334 66 33 91 34

This project has received funding from the Euratom research and training programme 2019-2020 under grant agreement No 945098.

| Project acronym<br>PREDIS | Project title<br>PRE-DISposal management of radioactive waste | | Grant agreement No.<br>945098 |
|---|---|---|---|
| Deliverable No.<br>D4.3 | Deliverable title<br>**Development of vacuumable gel decontamination processes** | | Version<br>1.0 |
| Type<br>Report | Dissemination level<br>Public | | Due date<br>M42 |
| Lead beneficiary<br>CEA | | | WP No.<br>4 |
| Main author<br>Alban Gossard | Reviewed by<br>Abdesselam Abdelouas, IMT | Accepted by<br>Maria Oksa, VTT, Coordinator | |
| Contributing author(s)<br>Aditya Rivonkar (IMT), Richard Katona (SORC), Thomas Carey (NNL), Fabien Frances (CEA), Clara Penavayre (CEA), Hippolyte Pochat-Cotilloux (CEA), Gabriella Lucena (CEA) | | | Pages<br>49 |


Abstract

Metallic wastes are critical materials to decontaminate. They are produced in very large volumes and have different nuclear energy industry origins, such as the contamination of the primary circuit components within power stations, processing vessels at reprocessing plants or even hot cell walls and floors.

“Vacuumable” gels can be utilised to chemically decontaminate metallic waste components and have the advantage of producing secondary solid waste, only. This report describes the development of new vacuumable gel formulations and implementation processes performed within the PREDIS project, which had the overall aim to increase their range of application.

New gel formulations, inspired from the COREMIX (Chemical Oxidation REduction using nitric permanganate and oxalic acid MIXture) process, were initially developed and their decontamination capability demonstrated and compared to a commercial product, Aspigel 100E from the FEVDI Company. Although the COREMIX-based gels were found to be less efficient, they offer an alternative in situations where the commercial product cannot be used (e.g. due to waste acceptance compatibility etc.) or for soft surface decontamination operations.

New processes were then developed for the decontamination on small objects with complex geometries (such as pipes, valves or pump) or limited access surfaces. Particularly, “magnetic gels” were formulated to be applied using magnet. Indeed, by adding ferromagnetic particles in their formulations, the gels can be spread by attraction with a magnet, allowing their deposition on surfaces non-accessible by spraying. A direct relationship between the amount of ferromagnetic particles, the rheological and spreading properties, and the gel decontamination efficiency was highlighted, paving the way to the development of even more optimized formulations.



Coordinator contact

Maria Oksa
VTT Technical Research Centre of Finland Ltd
Kivimiehentie 3, Espoo / P.O. Box 1000, 02044 VTT, Finland
E-mail: maria.oksa.@vtt.fi
Tel: +358 50 5365 844





Acknowledgement

This project has received funding from the Euratom research and training programme 2019-2020 under grant agreement No 945098.

# TABLE OF CONTENTS

# 1 Introduction

## 1.1 Context

The decontamination of solid surfaces is an important issue in the nuclear industry, notably for dismantling, decommissioning or maintenance tasks. Appropriated decontamination techniques are necessary to better handle the different waste generated through such operations. Particularly, decontamination is required to reduce the activity associated with certain forms of waste and minimize the waste volumes requiring long-term storage. The diversity of the materials involved is making these decontamination operations increasingly laborious and specific. Among them, metallic wastes are critical materials to decontaminate. They are produced in very large volumes and have different origins, such as the contamination of the primary circuit components within power stations [1], processing vessels at reprocessing plants [2] or even hot cell walls and floors. Thus, different surface geometries have to be considered such as large, flat walls but also small items with complex geometries such as pipes, valves or pumps. The main metallic surfaces to decontaminate are made of carbon steel, stainless steel and Ni-alloys (e.g. Inconel). Due to their contact time with strongly corrosive solutions (such as concentrated nitric acid for example) at high temperatures and pressures, these surfaces can be contaminated to a depth of a few microns [3]. Radioactive isotopes can be physically adsorbed on to surfaces or incorporated in the surface oxide layers [2]. Consequently, the decontamination of such surfaces needs the elimination of the corroded surface layers to remove the contamination from the bulk material. Different technologies have thus been developed over the years mainly consisting in physical decontamination (high pressure water, ultrasonic techniques…) or chemical decontamination (use of liquid reagents, gels/foams technologies, electrochemical techniques…) processes [3].

The work described in this report is based on a chemical decontamination technology referred to as a “vacuumable gel”. In the frame of the PREDIS project, a review article on the use of complex fluids for the nuclear decontamination was published [4], which described the “vacuumable” gel technology in detail. A short description is given below.

## 1.2 Description of the “vacuumable” gel technology

Vacuumable gels are inorganic and self-drying gels mainly developed at the CEA, France [4]. Such gels are composed of mineral colloidal particles (typically silica or alumina) dispersed in a decontamination solution. Due to their viscoelastic properties, the gel adheres to surfaces and forms a thin layer, which induces a prolonged contact between the surface and the decontamination gel. This solution specifically formulated to attack the substrate down to few tens of microns and then release incrusted contaminants, which are absorbed into the gel. Finally, the gel dries and fractures into a non-powdery solid, trapping the contamination that is readily removable by brushing or vacuuming. The Figure 1 describes schematically the principle of this technology.

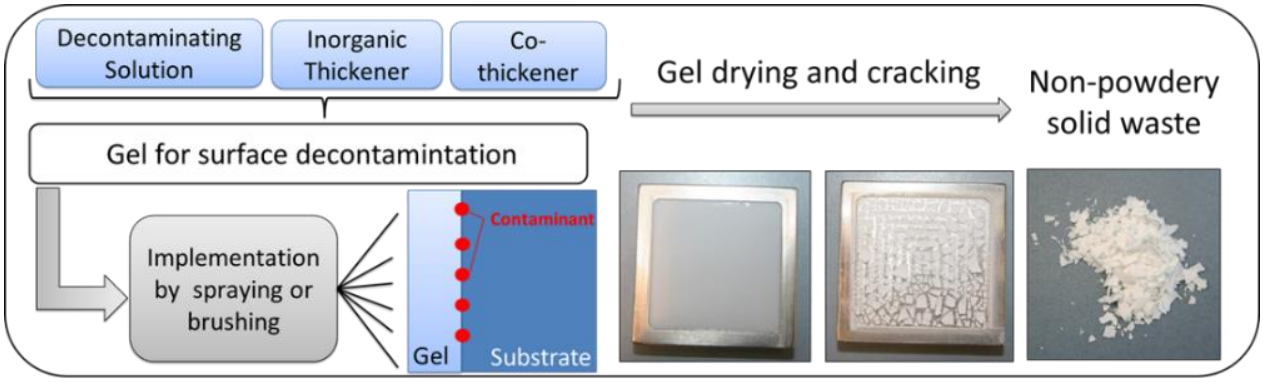


*Figure 1. Schematic representation of the vacuumable gel technology [4].*

One of the main advantages of this technology is that it decontaminates both the surface and the sub-surface without degrading the mechanical properties of the substrate. This can be controlled by adapting the chemical formulation of the gel. Such chemical compositions are relatively well known for the decontamination of metals (acid and oxidizing chemicals). Moreover, this process only produces inorganic solids waste, which are chemically inert, at the end of the operation, meaning that there is no secondary liquid effluents that have to be treated. These wastes are produced in a quite small amount (around 150 g of secondary waste per $m^2$ for a metallic surface) and can be directly conditioned and stored without any post-treatment.

Spraying of the gel is their most popular mode of implementation. For that, the gels must have shear thinning features, meaning that their viscosity decreases strongly under shear. This makes the gels liquid-like to apply by pumping and spraying at high speed through a nozzle. Moreover, the gels must become viscous again in a few seconds after spraying to adhere and not flow once spread on vertical surfaces. The Figure 2 presents pictures of a decontamination operation involving stainless steel (SS) surfaces.

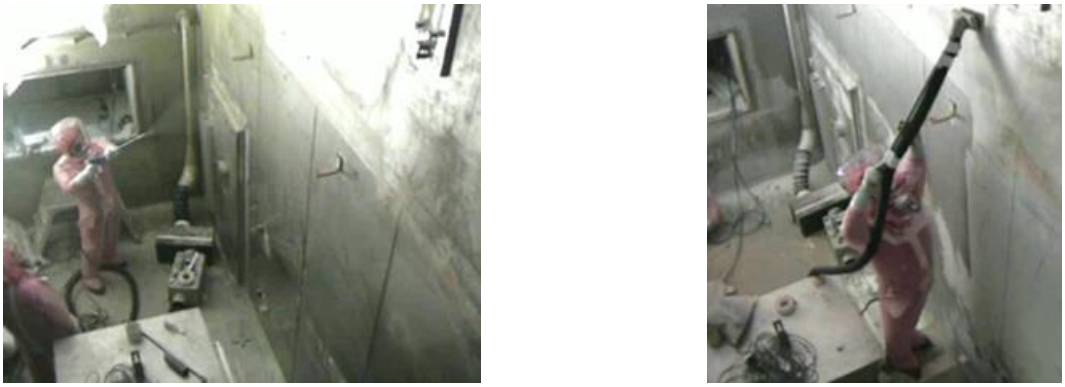

*Figure 2. Spraying of a vacuumable gel on a SS surface (left) and vacuum cleaning of the solid waste after drying (right).*

The gel is first sprayed on the surface using dedicated devices (Figure 2, left). The spraying devices are designed to pump the gels through specific nozzles, ensuring that the contaminated surface is covered homogeneously. After the gel decontaminates the surface and dries, the resulting solid residues can be recovered by vacuum cleaning (Figure 2, right). The main advantages of this implementation mode are that the devices are easy to handle and that the operator does not have to approach close to the contaminated surface.

## 1.3 Development performed during the PREDIS project to increase the application field of vacuumable gels

During the PREDIS project, the work aimed to evaluate the possibility to use vacuumable gels in different situations to increase their field of application. For that purpose, two main objectives were defined and are detailed below.

### 1.3.1 Efficiency on different corroded surfaces

Mature formulations of vacuumable gels exist and are commercialized under the name of Aspigel by the FEVDI Company (https://fevdi-nuclear.com/). First, the decontamination efficiency of such gels was characterized on different SS surfaces. These surfaces were specifically prepared to present different surface morphologies, i.e. presenting a more or less oxidative state. Moreover, an alternative gel formulation, inspired from the CORD process, was also developed and its efficiency was demonstrated and compared to the commercial product.

### 1.3.2 Application of the gels on items having complex geometries

“Sprayability” is an important property for vacuumable gels designed to treat large and plane surfaces such as the walls or floors of contaminated rooms. However, spraying is clearly not an option for small objects with complex geometries such as pipes, valves or pump. To use the gel technology for such items, two application processes were studied. The first application consists in using the gel as a bath, allowing to dip the contaminated items in it and leave a thin gel layer on the all surface.

The second one requires a modification of the gel formulation. By adding ferromagnetic particles to gel formulations, we have demonstrated that the gel can be moved and spread on non-accessible surfaces (such as the internal surface of pipes for example) using a magnet. This new process was patented during the PREDIS project [5] and the experiments performed for its development are described in this report.

# 2 Decontamination efficiency of gels on different corroded stainless steel surfaces

## 2.1 Evaluation of a commercial gel for the decontamination of stainless steel

### 2.1.1 Identification of an efficient commercial gel

The FEVDI Company has commercialised a range of Aspigel products, whose efficiency depends on the surface on which they are applied. Three different Aspigel products to decontaminate a SS coupon were identified. These were assessed using the efficiency evaluation protocol used to assess the different gels is as follows:

- The gels were deposited on coupons of SS 316 L with a known area and with a controlled thickness of 1 mm.
- The gels were let to dry for a few hours until the formation of solid residues.
- Solid residues were recovered by brushing and the coupons were washed with water and ethanol.
- The attacked thicknesses of the coupons by the gels were determined by mass loss comparison (before and after the gel) using the Equation 1:
-

Equation 1 $$Corroded\ depth = \frac{\Delta m}{S \times d}$$

Where $\Delta$m is the mass loss, S is the area covered by the gel and d is the SS density (fixed at 8 g.cm$^3$).

The composition of these gels are not exactly known, but their safety data sheets (https://fevdi-nuclear.com/) allowed to note the main component of their decontamination solution. Table 1 details the gel compositions and the results from the assessment. The different steps of the evaluation protocol are illustrated by the Figure 3.

Table 1. Efficiency of different Aspigels on SS samples.

| Gel name | Decontamination solution | Deposited layer thickness | Attacked SS thickness |
|---|---|---|---|
| Aspigel 200 | Citric acid + phosphoric acid | 1 mm | 0.02 µm |
| Aspigel 400 | Nitric acid + phosphoric acid | 1 mm | 0.004 µm |
| Aspigel 100E | Nitric acid + Ce(IV) | 1 mm | 0.24 µm |
| Aspigel 100E | Nitric acid + Ce(IV) | 5 mm | 1.1 µm |

*Figure 3. Decontamination of a SS coupon using Aspigel 100E.*

Aspigel 100E demonstrated the best efficiency to decontaminate a SS surface due to both the effect of the Ce(IV) as a strong oxidant and nitric acid facilitating the dissolution of the metallic surface. Note that these results are well in accordance with the preconisation of the FEVDI Company (https://fevdi-nuclear.com/).

In a subsequent experiment, the influence of the gel thickness on the efficiency of the Aspigel 100E was investigated using a similar procedure to the one described above but with a gel layer of 5 mm. After drying, the SS coupon was attacked to a depth of 1.1 µm (see Table 1). Indeed, a thicker layer of gel enabled a larger volume of decontamination solution to be applied to SS coupon and for a longer contact time. However, we note that the rheological properties of the vacuumable gels limit their possible thickness deposition on vertical surfaces at only 1-2 mm. Consequently, large thicknesses of gels can only be used on horizontal (or at least non-vertical) surfaces.

To conclude, this study determined that the best Aspigel product to be used on SS coupons was the Aspigel 100E, with an efficiency evaluated to few tens of microns depending on the deposited gel thickness.

### 2.1.2 Coupling electrochemistry and mass loss to better understand the gel decontamination mechanism

A better understanding of the gel decontamination mechanism may help to develop new formulations and improve their efficiency. For that purpose, a methodology was established by coupling mass loss measurements and electrochemical characterization.

Aspigel 100E was used as a model gel and an austenitic SS 1.4571 (316 grade), containing chromium and nickel, as a model substrate. The SS 1.4571 composition is given in Table 2.

*Table 2. Composition of the SS 1.4571 coupons.*

| | | | | | |
|---|---|---|---|---|---|
| Element concentration [%] | C | Si | Mn | P | S |
| | 0.08 | 1 | 2 | 0.045 | 0.015-0.03 |
| | Cr | Ni | Mo | Ti | Fe |
| | 16.5-18.5 | 10.5-13.5 | 2-2.5 | 0.4-0.7 | Balance |

#### 2.1.2.1 Evaluation of the corrosion rate considering an "infinite" contact time (no dyring of the gel) by electrochemical tests

A three-electrode electrochemical cell was used to measure the corrosion rate of the SS when immersed in Aspigel 100E. This evaluation is theoretical and assumes that the contact of the gel with the SS is "infinite", meaning that no drying occurs during the operation. A Radelkis OP-0830P saturated calomel reference electrode (SCE), A SS counter electrode and the SS 1.4571 coupons, as the working electrode, were immersed in a bath of the Aspigel 100E. The working electrode was a disc with a diameter of 1.5 cm. Prior to measurements, the discs were ground to 180 grit with emery paper and the open circuit potential (OCP) was measured for 5 min. The electrochemical cell was connected to Voltalab PGZ201 potentiostat and the working electrode was polarised at a sweep rate of 1 mV/s. The potential range was +/- 200 mV. According to the Butler-Volmer equation, the polarisation curve is as followed [6]:

Equation 2

$$i=i_0\left(e^{\frac{\beta z_a F}{RT}\Delta E}-e^{-\frac{\alpha z_k F}{RT}\Delta E}\right)$$

Where i is the current density (mA.cm$^{-2}$), $i_0$ is the equilibrium current density (mA.cm$^{-2}$), α/β are the oxidation/reduction factors, $z_a/z_k$ are the amount of the change in charge numbers, F is the Faraday constant, T is the temperature, R is the universal gas constant and ΔE is the polarisation (mV).

Successive polarisation curves of the SS 1.4571 in Aspigel 100E are shown in Figure 4.

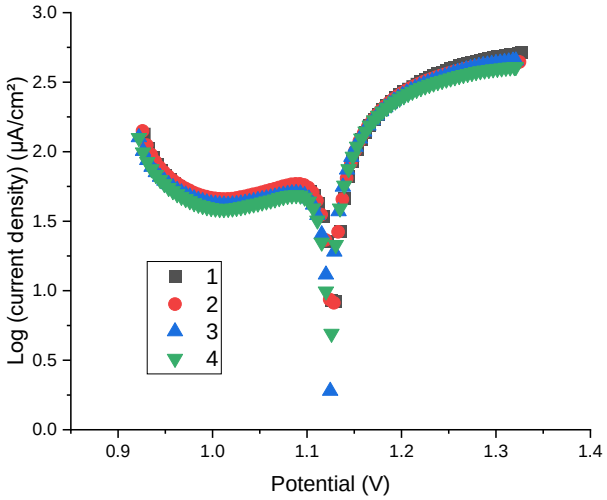


*Figure 4. Successive polarisation curves of a SS 1.4571 coupon using Aspigel 100E.*

The potential and the equilibrium current densities were determined by Tafel extrapolation. The corrosion rate, CR (mm/year) was calculated from Equation 3:

Equation 3 $$CR = i_0 \cdot \frac{M}{z} \cdot \frac{10}{d \cdot F}$$

where M the molar mass (g.mol$^{-1}$) and d the density of the metal (g.cm$^{-3}$).

The calculated corrosion current densities and the corrosion rates are summarised in Table 3.

*Table 3. Calculated data obtained from the electrochemical results.*

| | $i_0$ | CR |
|---|---|---|
| | [µA.cm$^{-2}$] | [mm/year] |
| 1 | 305.08 | 3.48 |
| 2 | 332.19 | 3.79 |
| 3 | 293.74 | 3.35 |
| 4 | 284.81 | 3.25 |

**The average corrosion rate was calculated as 3.47 +/- 0.23 mm/year**. Moreover, a peak is observed in the cathodic part of the polarisation curves, which we assume to be a reduction of Ce(IV) ions induced by the reaction with the SS surface. After the Ce (IV) ions had oxidised the metal, the acid cleans the surface by dissolution, which is highlighted by the polarisation curve characteristics of the anodic part.

#### 2.1.2.2 Evaluation of the stainless steel dissolved thickness as a function of the Aspigel 100E-SS contact time

SS 1.4571 substrates were prepared by first polishing and cleaning (with water and ethanol) to obtain a smooth and non-oxidized surface. Samples were dipped in a bath of gel to deposit a millimeter thick gel layer on the coupons. Then, the contact between the gel and the SS was varied from few hours until gel drying. At each pre-defined contact time, the residual gel (or solid residues in case of complete drying) was removed from the coupon. The samples were washed again (water and ethanol) and the mass loss of the SS sample was measured. From these experimental values, the dissolved SS thickness was calculated using Equation 1 as well as the corrosion rate using Equation 4.

Equation 4 $$CR = \frac{\Delta m}{surface.density.contact\ time}$$

Where Δm is the mass loss.

The results are reported in Figure 5.

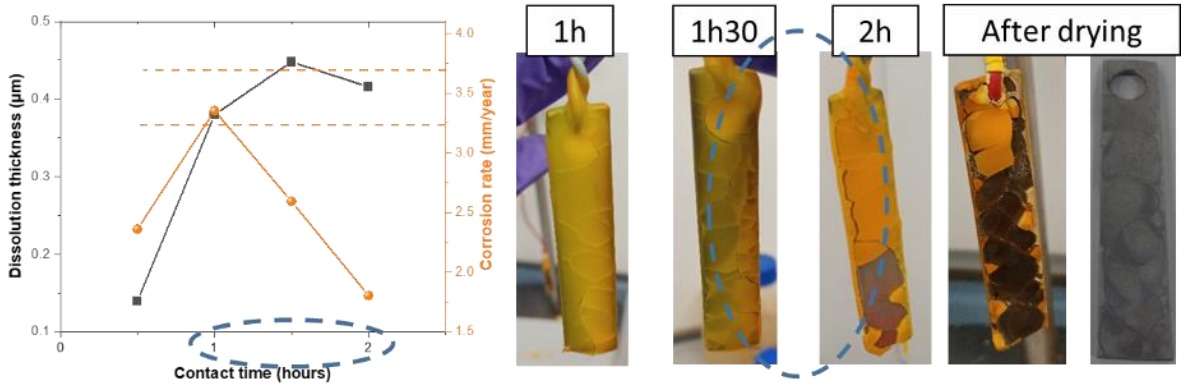


*Figure 5. Evolution of the dissolution thickness of the SS after gel application as well as the calculated corrosion rate as a function of the Aspigel100E – SS 1.4571 contact time and associated pictures.*

During the first hour, the dissolved metal thickness increases with the contact time until reaching few tens of microns. More interestingly, **the corrosion rate determined from this mass loss evaluation is consistent with the corrosion rate obtained from electrochemical tests**, i.e. between 2.5 and 3.3 mm/year. Then, the dissolved thickness of the SS coupon does not increase any more with time, while the corrosion rate drastically drops. This decrease can be explained by the drying of the gel, which induces cracks and formation of solid residues from one hour of drying approximately, inducing a decrease of the contact area between the gel and the SS substrate. This phenomenon is even more marked because the samples were hanged out, simulating the decontamination of a vertical surface, and the drying residues detached from the substrate. Consequently, from this point, the evaluation of the dissolution thickness and corrosion rate is not pertinent anymore due to this modification of the contact area.

Note however that the mass loss still increases until final drying of the gel. This suggested that the dissolution of the metal continued where the Aspigel remained in the contact with the SS, causing a slight inhomogeneous dissolution thickness. This observation was enhanced by the vertical orientation of the SS coupons, inducing a loss of some part of the gel during drying. Decontamination on a horizontal surface would make this less visible. Complementary SEM observations could be used to complete these data and illustrate the surface topography before and after decontamination.

Figure 6 shows the XRD data collected for the SS samples before and after the deposition and drying of Aspigel 100E.

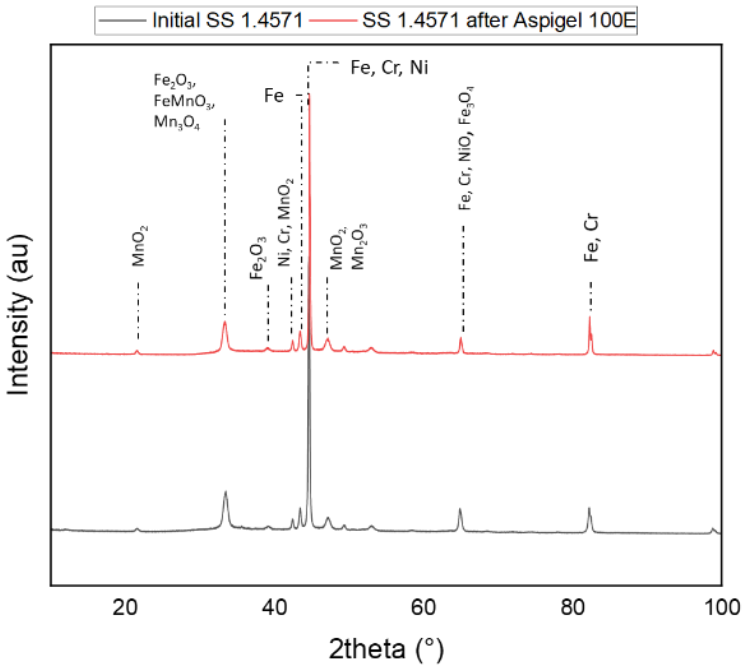


*Figure 6. X-ray diffractograms of the SS 1.4571 samples before and after Aspigel 100E decontamination.*

No significant modification of the metallic surface composition following the decontamination operation is observed. The Aspigel 100E does not modify the crystallographic structure of the SS after decontamination. Only a weak oxidation of the metal occurs, and explains the slight color changing visible on Figure 5, which can be highlighted by the SEM images and EDX analyses presented Figure 7.

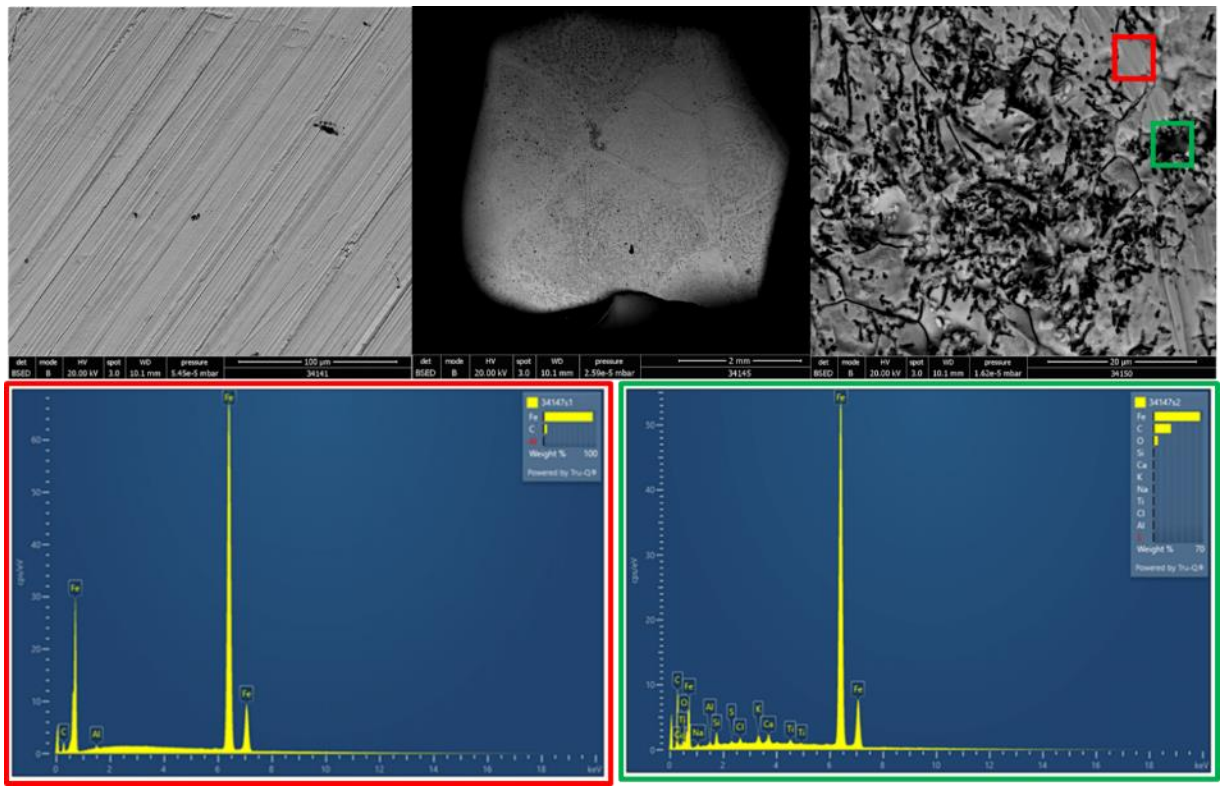

*Figure 7. SEM images of different magnifications of the SS samples before (left) and after (center and right) the deposition and drying of Aspigel 100E, and associated EDX analyses.*

The SS sample before decontamination is smooth and homogeneous, with only the presence of scratches coming from the polishing step. The image at a large magnification of the SS after the Aspigel 100E deposition shows in more detailed the inhomogeneous morphology visually observed in Figure 5. Some parts of the metallic sample seem more attacked by the gel than other, which can be explained by the drop of barely dried gel pieces not very well adhered anymore on the substrate. This leads to different contact time between the gel and the SS samples and the presence of “open” zones, which are differently corroded. Nevertheless, the different scratches are not observed anymore, proving the elimination of a metallic layer by the gel on the whole sample.
Then, more locally, EDX analyses were performed on a “grey” and smooth zone and a darker and rough zone. The first zone is mainly composed of iron, while the second one contains more oxygen. This is consistent with a surface having different local morphologies and compositions, with the presence of more or less oxidized zones due to the reaction with the Aspigel 100E.

#### 2.1.2.3 Conclusion

Electrochemical characterization and mass loss measurements have been coupled to highlight the Aspigel decontamination efficiency on SS 1.4571 samples. Thus, a corrosion rate comprised between 2.5 and 4 mm/year has been determined in a case of an “infinite” contact between the gel and the substrate, i. e. if the gel never dries. However, as soon as the first cracks appear during drying, the surface of contact between the gel and the SS substrate decreases, particularly in the case of a vertical surface because dried part of the gel may fall by gravity. Consequently, some inhomogeneities may be induced but, despite that, the dissolution of few tens of microns already occurred during the first hour (before drying), which is enough to decontaminate the metallic surface on this thickness. Note that this phenomenon is certainly less marked on a horizontal surface but will nevertheless occur at some time or another.

### 2.1.3 Evaluation of the Aspigel 100E for the decontamination of a strongly corroded SS sample

The efficiency of the Aspigel 100E was also evaluated on strongly oxidized SS samples. Such samples were prepared by SORC by contacting SS coupons with a flow of water vapour at 800°C during 8 hours forming a thick multi-layered corrosion of approximately 6 µm depth, mimicking a metallic surface from the primary circuit component [1]. Then, a 1 mm thick layer of Aspigel 100E was deposited on these coupons until gel drying. The Figure 8 on the left shows pictures of the different steps of the experiment.


*Figure 8. Decontamination of strongly oxidized SS samples by Aspigel 100E: one application (top), and successive applications (down).*

The results were less satisfying than for non-oxidized SS samples. The mass loss of the coupons was 99.2 ± 1.0 mg but, as visually observed, the sample attacked by the gel was not homogenous. XRD analyses were performed on the strongly oxidized SS samples before and after decontamination using Aspigel 100E and results are given in Figure 9.

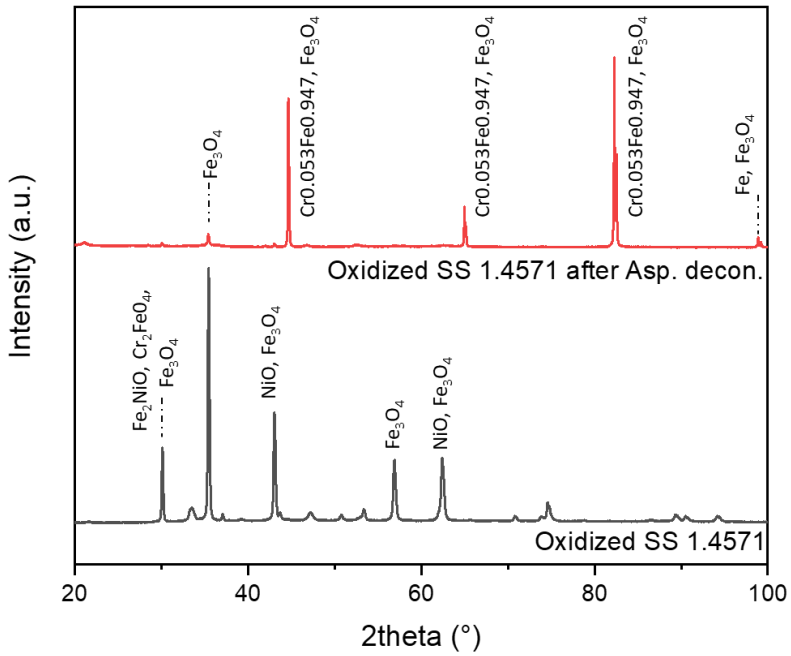


*Figure 9. X-ray diffractograms of the oxidized SS 1.4571 samples before and after Aspigel 100E decontamination.*

The oxidized SS 1.4571 sample presents various oxides of Ni, Fe and Cr. Then after decontamination with Aspigel 100E, some peaks of iron oxides are still quite visible with small Cr, which is consistent with the visual observation of the formation of an orange layer. Cr and Ni enriched layer are thus mainly dissolved and extracted by the Aspigel 100E, while strong Fe enriched layer remain on the substrate. Indeed, notably due to the drying of the gel and as illustrated above, the chemical reaction may be inhomogeneous at the surface of the SS and time may be missing for the decontamination solution to dissolve the strong Fe enriched oxide layer. Thus, two other successive applications were then tested to try to improve the coupons decontamination. However, as illustrated on the right picture of the Figure 8, the efficiency is not very much better. A solution to improve the decontamination efficiency could be the use of another chemical solution better able to quickly dissolve the oxidized layer before drying.

### 2.1.4 Conclusion

Aspigel 100E was determined as an efficient gel to decontaminate SS substrates. A corrosion rate around 3-4 mm/year (in case of an infinite contact time, i.e. without drying) was determined and allows the decontamination of SS surfaces on few tens of micron during the first hour of contact. However, the gel decontamination performances drastically decrease on strongly oxidized samples, notably when the oxide layer is thicker than a few microns.

## 2.2 New vacuumable gel formulations based on the COREMIX process

In order to have a vacuumable gel more efficient on strongly oxidized samples, new gel formulations were developed by modifying the nature of the chemical decontamination solution.

### 2.2.1 Presentation of the chemical solutions

The COREMIX (Chemical Oxidation REduction using nitric permanganate and oxalic acid MIXture) process, inspired from the CORD process, involves to two successive reaction steps. The first one

consists in using a solution containing permanganate ions ($MnO_4^-$), either in nitric acid or in alkaline media, to oxidize the chromium oxide layer:

$$Cr_2O_3 + 2MnO_4^- + H_2O \rightarrow 2HCrO_4^- + 2MnO_{2(s)}$$

Then, a second oxalic acid solution is used to reduce $MnO_4^-$ to $Mn^{2+}$ and to dissolve the Fe enriched oxide layer:

$$Fe_3O_4 + 4H_2C_2O_4 \rightarrow 3FeC_2O_4 + 2CO_2 + 4H_2O$$

Such a process may be repeated several times for an efficient decontamination, but induces large amount of liquid secondary waste to be post-treated [1].

In the frame of the PREDIS project, the efficiency of this technology was studied at IMT Atlantique to optimize the process performances in term economic, technical and safety purposes [1]. Then, two chemical compositions of decontamination solutions were identified to be integrated in vacuumable gel formulations:

- A first oxidative solution containing 15 mmol.L$^{-1}$ of $KMnO_4$ and 3 mmol.L$^{-1}$ of $HNO_3$.
- A second reductive solution containing 18.5 mmol.L$^{-1}$ of oxalic acid.

### 2.2.2 Incorporation of the COREMIX-based chemical solutions in a vacuumable gel

Two strategies were tested to incorporate COREMIX chemical solutions in vacuumable gels.

- Approach 1: addition of the decontamination reagents in a pre-formed $H_2O$-silica gel

For safety reasons, we tried to limit the direct manipulation of nanoparticles (NPs). Thus, the first experiments were performed on a commercial gel containing 16 wt% of silica (Aerosil®380, Evonik Industries) dispersed in water purchased at FEVDI. This gel was very viscous before the addition of the chemical reagents. Chemical reagents were directly added to the gels, which were then vigorously mechanically stirred with a three-blade stirrer for homogenization. However, whatever the gel composition ($KMnO_4$ - $HNO_3$ or oxalic acid), a drastic loss of the gel viscosity was observed and the gels became too liquid to be used. Indeed, aqueous slurries made of silica particles may behave like sols or like gels depending on the particle concentration, but also on the pH or the ionic strength of the medium [7]. With acids particularly, care has to be taken due to the pH influence on the particles surface charges and, in turn, the interaction between them, directly affecting the formation and stability of the gel structure, and consequently its viscosity [8]. That is why, silica NPs had to be added any way in the gel formulations to maintain a high viscosity. The formulation protocol is schematically described Figure 10.

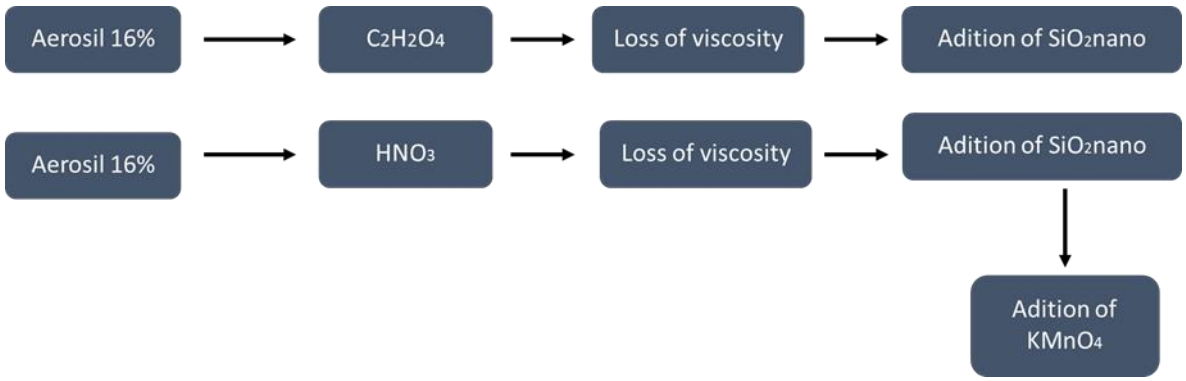


*Figure 10. Approach 1 to formulate vacuumable gels based on the COREMIX decontamination process.*

We first prepared gels from the silica-$H_2O$ commercial gel with the correct amounts of acid, obtaining almost liquid gels as described above. Then, we added to these gels silica NPs (using Aerosil®380, Evonik Industries) until an adapted viscosity was visually obtained. The oxidative gels were finally completed with the necessary amount of $KMnO_4$. The different tested formulations are given in Table 4.

*Table 4. Formulations of decontamination gels based on the COREMIX decontamination process realized with the approach 1.*

| Type of gel | | Concentration in $SiO_2$ (%wt) | | | | |
|---|---|---|---|---|---|---|
| $KMnO_4$ | $HNO_3$ | 20 | 21 | 22 | 23 | 24 |
| 3 mM | 15 mM | | | | | |
| $C_2H_2O_4$ | | 24 | | | | |
| 18.5 mM | | | | | | |

Figure 11 show the visual oxidative gel textures having 20-24 %wt in $SiO_2$. The oxidative gel containing 24 %wt in $SiO_2$ presents a “wet sand like” texture not adapted to the process. This was not observed for the 21, 22 and 23 %wt $SiO_2$ containing gels but they remained extremely viscous. The 20 %wt in $SiO_2$ containing gel appears however to be very liquid. Then, after three days, the 20% gel became solid-like, as shown in the Figure 11. This behavior could be explained by the reorganization with time of the particles in solution after the mechanical mixing due the thixotropic feature of the silica-based gels. Consequently, the texture of the gels is difficult to control using this synthesis protocol and none seems to be adapted to be used as a decontamination gel.

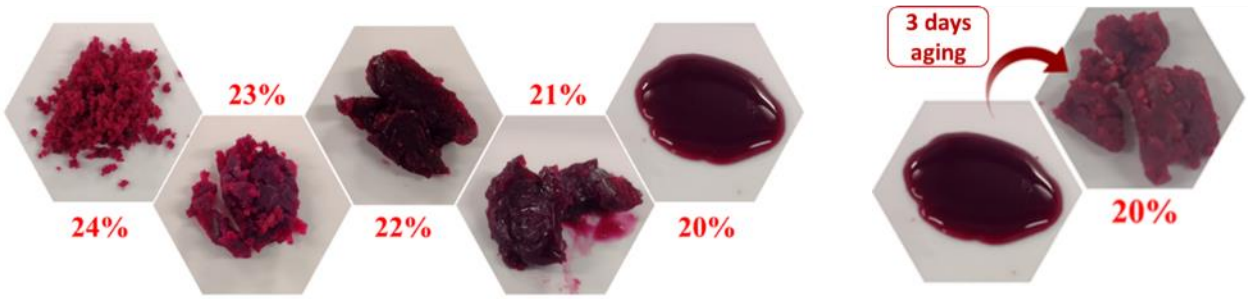


*Figure 11. Pictures of the oxidative gels having 20-24 %wt in $SiO_2$ (left) and of the time evolution of the 20 %wt $SiO_2$ containing gel after 3 days aging (right).*

The oxalic acid based gel was formulated in the same way and an optimal viscosity was visually obtained with a content of 24 %wt silica, as shown in Figure 12. This formulation showed promise because the initial gel was quite viscous and the viscosity decreased after mechanical shearing.

Rheological characterization was then performed. An initial shearing rate of 50 $s^{-1}$ was applied to the gel to make it liquid as required during the application of the gel by spraying or manual deposition. Then, a shear rate of $5.10^{-3}$ $s^{-1}$ was immediately imposed to simulate the gel at rest after application. Figure 12 shows the evolution of the gel viscosity during this process.

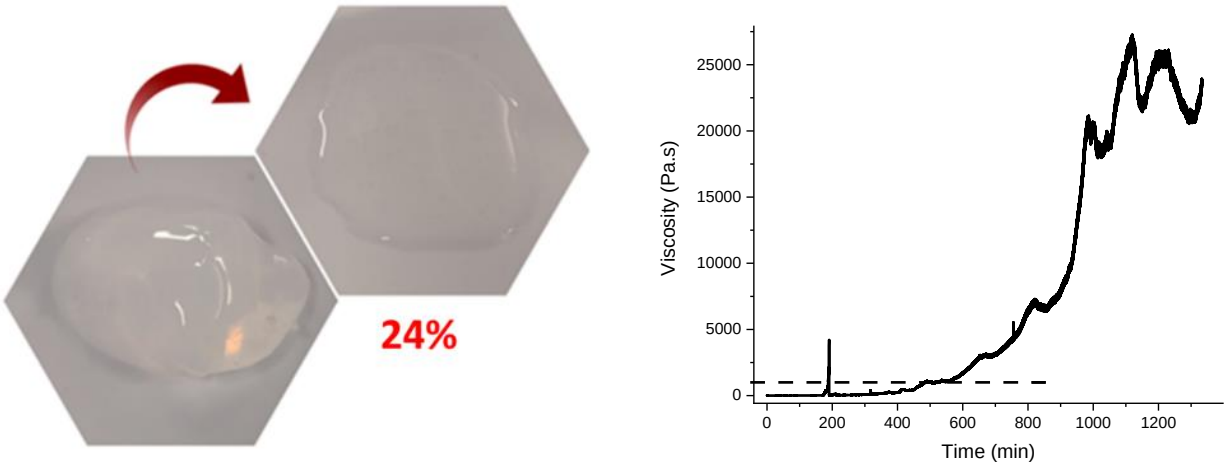


*Figure 12. Oxalic acid based gel containing 24 %wt $SiO_2$ before and after mechanical mixing (left) and its rheological analysis (right).*

The viscosity recovering of the oxalic acid based gel containing 24 %wt $SiO_2$ is very long. Indeed, a viscosity of 1000 Pa.s is obtained after around 500 minutes. This property is not well adapted for the gel to be used because a too low viscosity directly after application will induce a flow of the gel. Moreover, after the rheological experiment, the gel was not homogeneous anymore with several large aggregates, meaning that the gel does not remain stable after shearing.

To conclude, this first approach to formulate new gels was not optimal. Indeed, the gels was not stable with time or under shearing certainly because they are non-homogeneous. As the surfaces of the particles are modified by the complex environment of the solution, there are consequences on the phenomena of attraction/repulsion between particles and thus on the behavior of the gels. A commercial gel having its own stability is used at first. Then, adding chemicals modifies a first time the particles interactions in the gel. Moreover, the new silica NPs (added to increase the viscosity) have their own interaction and may consequently induce an inhomogeneous network of viscosing agent. Note finally that the use of silica NPs we initially wanted to avoid for safety reason is necessary any way. That is why, a second approach was tested.

- Approach 2: addition of silica NPs directly to a decontamination solution

The second approach consisted in preparing first the liquid solutions containing the right chemical concentrations. Silica NPs were then progressively incorporated under mechanical shearing using a three-blade stirrer until a satisfying gel texture was obtained. Between 9 and 11 %wt of silica NPs were necessary to obtain an oxidative gel (containing $KMnO_4$ and $HNO_3$) and between 9 and 13 %wt for a reductive gel with oxalic acid. The Figure 13 shows pictures of such gels at rest and after a mechanical shearing. The different formulations appears visually satisfying to be used in a vacuumable gel process.

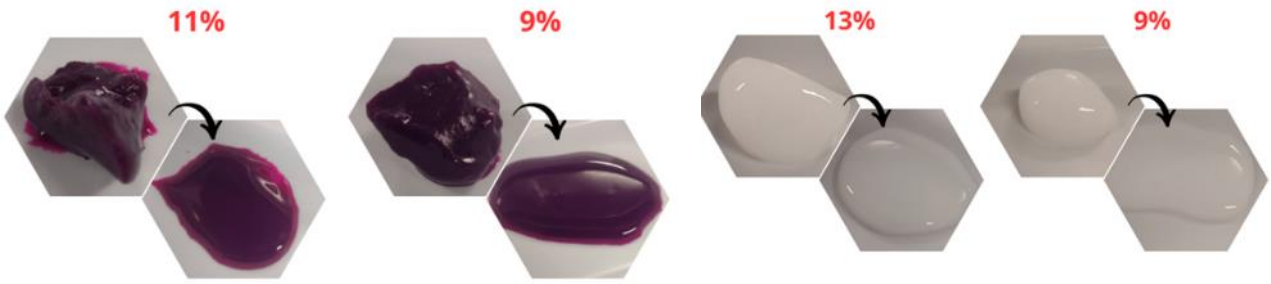


*Figure 13. Visual textures of different oxidative (left) and reductive (right) gels at rest and after a mechanical shearing.*

Rheological analyses were performed on the different formulations. After application of a shear rate of 50 $s^{-1}$ for 2 minutes, the evolution of the viscosity at a shear rate of $5.10^{-3}$ $s^{-1}$ (to simulate the gel at rest) was followed and is represented Figure 14.

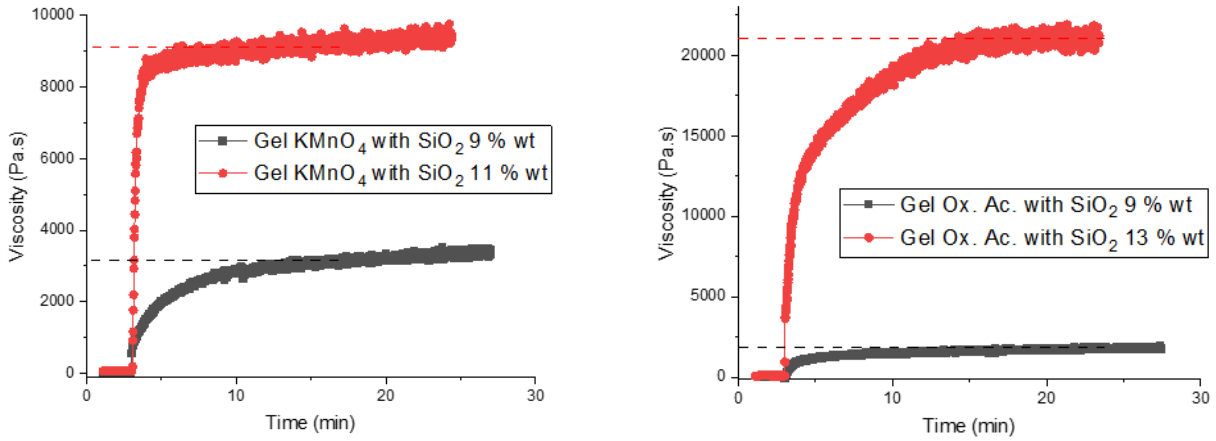


*Figure 14. Evaluation of the rheological properties of the oxidative (left) and reductive (right) gels.*

As soon as the 50 $s^{-1}$ shearing step is stopped, the viscosity immediately increased and a plateau was reached after only around 10 minutes. The values of the viscosity plateau increased with the content of silica NPs, from a few thousands of Pa.s for gels with 9 wt% in silica NPs to more than 20 000 Pa.s for the reductive gel having 13 %wt in silica NPs. These values are consistent with a possible application of a thin gel layer on metallic surfaces, even vertical. Moreover, the gel texture remains homogenous even after some successive shearing steps.

- Composition of the final gels

Finally, the approach 2 was used to formulate vacuumable gels based on the COREMIX process. Two gels have been identified to test their decontamination efficiency:

- An oxidative gel containing 9 %wt in silica NPs and a decontamination solution consisting in 15 $mmol.L^{-1}$ of $KMnO_4$ and 3 $mmol.L^{-1}$ of $HNO_3$.
- A reductive gel also containing 9 %wt in silica NPs and a decontamination solution consisting in 18.5 $mmol.L^{-1}$ of oxalic acid.

These silica weight percentage were chosen because they are sufficiently high for the gel to present adapted rheological properties and because this amount of silica will induce a lower amount of secondary waste as well as a larger volume of decontamination solution.

### 2.2.3 Evaluation of the new gel formulations

The decontamination performances of the gels formulated from the COREMIX process were evaluated on SS coupons oxidized with different protocols.

#### 2.2.3.1 On slightly oxidized coupons

- Preparation of the samples

316L SS samples were treated using 1 M HCl to obtain a thin layer of corrosion for the gel decontamination efficiency tests. After polishing, samples were thus immersed in a 1 M HCl solution in contact for 1 h, 2 h, 4 h, 5 h, 1 day, 2 days and 3 days (see Figure 15).

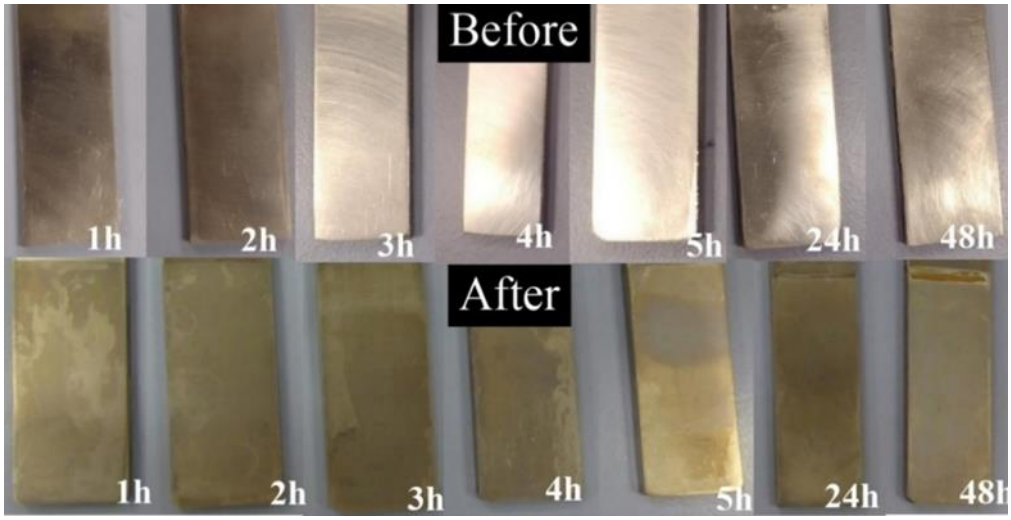


*Figure 15. Pictures of SS coupons before and after being oxidized in HCl 1 M during different times.*

Visual corrosion of the samples were observed (Figure 13). Note that pitting corrosion is most likely here, which is different to the corrosion mechanisms in the later coupons. The evolution of the sample mass loss was measured which allowed the determination of the corrosion rate, given in Figure 16 as a function of the contact time between the SS coupon and the HCl solution.

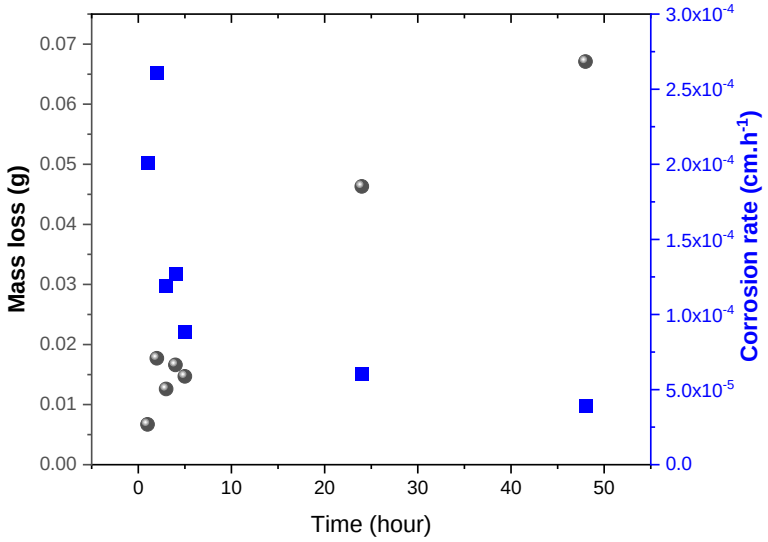


*Figure 16. Evolution with time of the mass loss of SS samples in an HCl 1 M solution and associated corrosion rate.*

The global evolution of the mass loss with time has a parabolic behaviour, even if small deviations are observed for low contact times, which could be explained by different initial surface states and morphologies due to the polishing step. This type of oxidation curve usually occurs in the formation of fine oxide layers at low temperatures. This is characteristic of a rapid oxidation occurring as soon as the contact between the metal and the acidic solution, until tending toward stabilization for long contact times [16, 17]. This is confirmed by the evolution of the corrosion rate with time. Indeed, the corrosion speed depends directly on the availability and mobility of zones and surface defects that enable oxygen transport through the layers. Wagner's theory predicts parabolic oxidation kinetics when the limiting step is the diffusion of oxygen ions through oxygen vacancies, where the driving force for transport is the oxygen activity gradient in the oxide layer.

To better understand the phase evolution of the SS surfaces and the corrosion mechanism, the HCl solution were analyzed by Inductively Coupled Plasma-Optical Emission Spectrometry (ICP-OES) after their contact times with the coupons. The evolution of some metal concentrations are represented Figure 17.

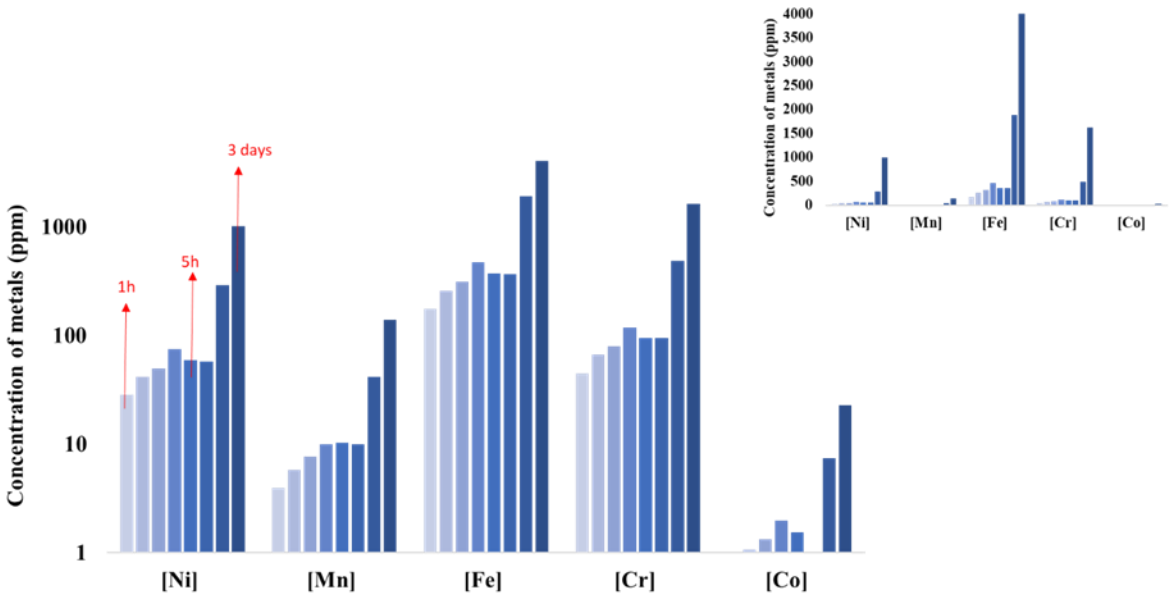


*Figure 17. Metal concentrations measured in ICP-OES present in each solution as a function of the contact time between a SS coupon and 1 M HCl. Insert are the same values in linear scale.*

The amount of metal in solution increased with the contact time. First, the increase was in accordance with the high mass loss and corrosion rate. Then, a plateau was observed from 4 to 24 hours. After 24 hours, a further increase was observed. This can be correlated with the visual observation of the coupons, on which the oxide layer is not very adhered any more on the SS substrate and start to take off the substrate. We can thus reasonably assume that large pieces of oxide layers detached from the substrate and dissolved, leading to higher concentrations of metals in solution. The linear plot of the data in the insert of the Figure 17 highlights that iron is mainly dissolved, but also nickel and chromium, which is consistent with the composition of the SS.

Finally, a contact time of 24 hours was concluded to be optimum. Indeed, the SS coupons were oxidized and the created oxide layer remained strongly attached. To verify the repeatability of the manipulation, a corrosion test was performed using 7 different SS samples submitted to the same acid concentration (1 M HCl) conditions for 24 hours. The mass loss was measured and the average and standard deviation were calculated obtaining, respectively, 0.046 +/- 0.013 g.

- Performances evaluation

The protocol used to evaluate the performance of the COREMIX-based gels is schematically described Figure 18.

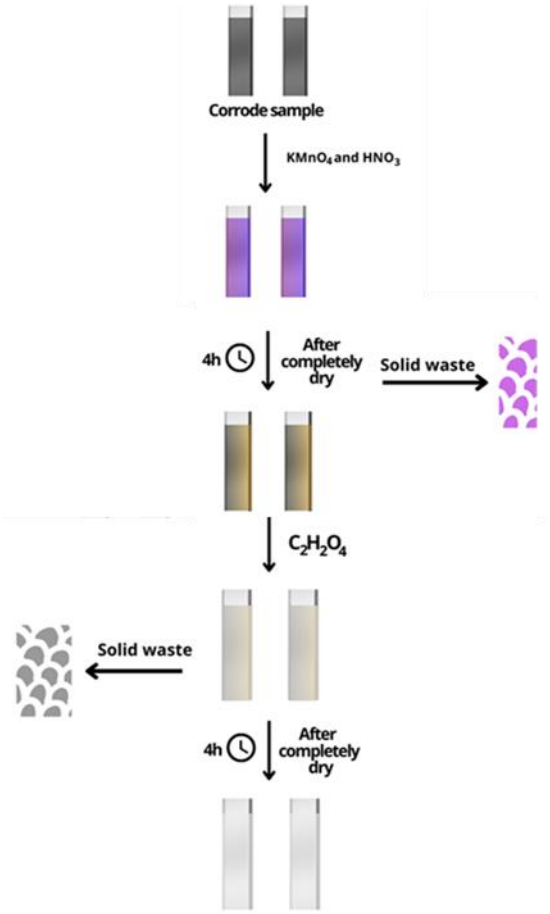


*Figure 18. Schematic description of the protocol evaluation of the COREMIX-based gels efficiency.*

First, the oxidative gel (containing $KMnO_4$ and $HNO_3$) was deposited on a SS coupons (oxidized 24 hours in 1 M HCl) with a millimetre thickness. After drying, solid residues from the gel were recovered by brushing. Then, a millimetre layer of the gel containing oxalic acid was deposited to perform the reductive step of the decontamination process. Solid residues were also removed after drying. Finally, both solid residues were separately dissolved in HF before elementary analysis by ICP-OES to determine the absorbed metal at each step of the process. The Figure 19 shows different pictures of such a decontamination operation using the gels based on the COREMIX process.

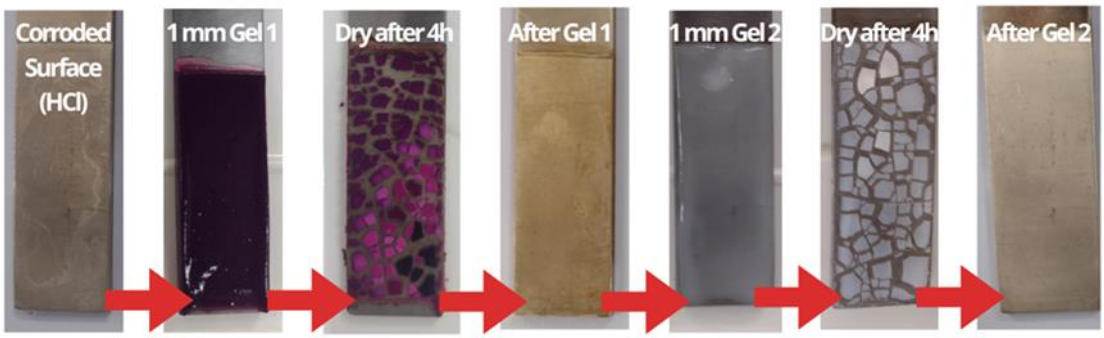


*Figure 19. Pictures of a decontamination operation of a slightly oxidized SS using the vacuumable gels based on the COREMIX process.*

By assuming that the density of the oxidized metal is close to the one of the SS, Equation 1 leads to a total (i.e. after the 2 gels application) corrosion depth of 0.08 µm, which is quite low but could be in the order of magnitude of the slightly oxidized layer. Figure 20 presents the metal (particularly Fe, Ni and Cr) concentrations determined by ICP-OES in the solid residues of the gel after their

dissolution. Note that the concentration values are indicative and can be interpreted only for a comparative evaluation.

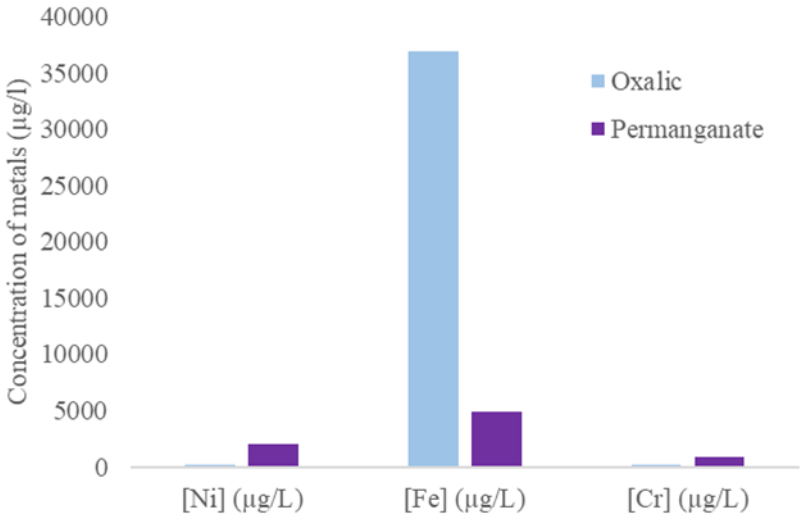


*Figure 20. Metal concentrations measured by ICP after dissolution of the solid residues of the oxidative (Permanganate) and reductive (Oxalic) gels.*

These results are consistent with the observation made by Rivonkar et al. [1] with liquid solutions. The first step with permanganate potassium oxidized the layer and remove a large part of Cr. Some Fe, which may be slightly dissolved due to presence of nitric acid in the formulation, are also absorbed by the gel. Then, the oxalic acid based gel strongly dissolves iron oxides, whose concentration in the solid residues drastically increases, while residual Cr have been detected. Interestingly, Ni seemed to be more dissolved in the first step than in the second one, because the Cr-enriched oxide layer also contains a large amount of Ni.

The performance of the commercial Aspigel 100E on these slightly oxidized samples was also evaluated using the protocol illustrated in Figure 18 and pictures are given in Figure 21.

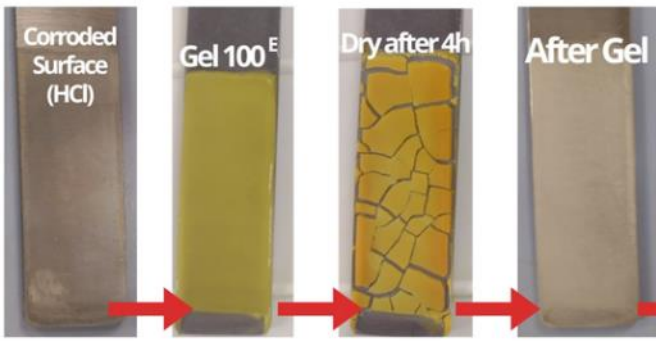


*Figure 21. Pictures of a decontamination operation of a slightly oxidized SS using Aspigel 100E.*

Mass loss measurements gave a corrosion depth about 0.60 µm, which is more important than with the COREMIX-based gels. Indeed, Aspigel 100E can dissolve a thin oxidized layer but also proved to be efficient on non-oxidized SS coupons (see above).

Scanning electron microscope (SEM) images were performed on coupons at different step of the process and are compared Figure 22 and Figure 23. Moreover, Energy Dispersive X-Ray Analysis (EDX) was done on different zones to analyse the chemical composition of the surfaces.

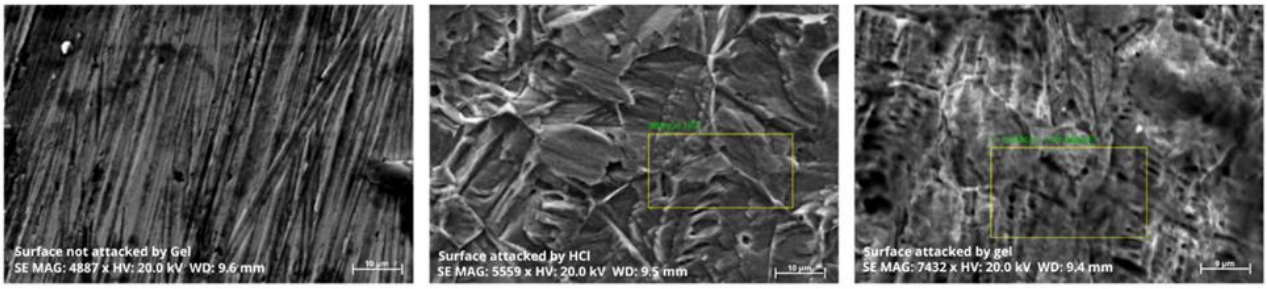


*Figure 22. SEM images of a SS coupon before and after the oxidation step (left and center) and after the decontamination process applied with the COREMIX-based gels (right).*

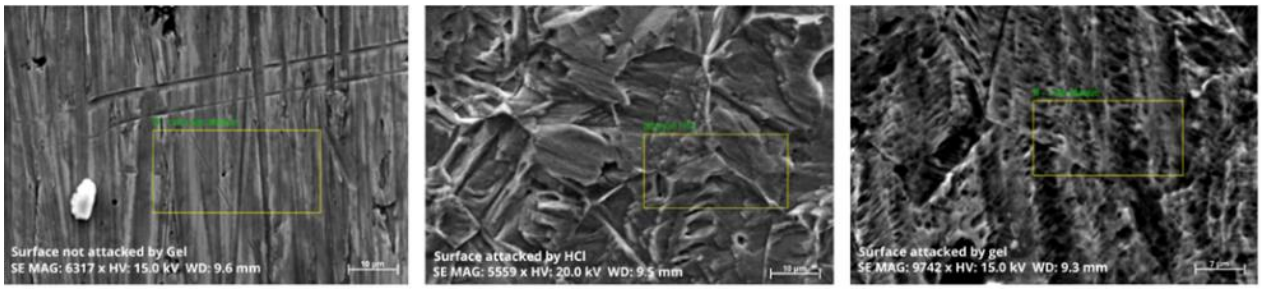


*Figure 23. SEM images of a SS coupon before and after the oxidation step (left and center) and after the decontamination process applied with the Aspigel 100E (right).*

The SS coupons before the oxidation step are relatively smooth with the presence of scratches coming from the polishing step. Then, after the oxidation in HCl, the surfaces are rougher and uneven, and the polishing scratches are not visible any more. This is a characteristic of the chemical reaction with HCl and the formation of the oxide layer. After the gel deposition, this oxide layer has been chemically attacked and its relief is smoother although it is still possible to distinguish it, notably after the COREMIX-based process.

The Table 5 gives the results of the EDX analyses.

*Table 5. Weight quantification by EDX of the elements at the surface of the SS coupons at different steps of the decontamination processes.*

| Sample | C (%wt) | O (%wt) | Fe (%wt) | Ni (%wt) | Cr (%wt) |
|---|---|---|---|---|---|
| Surface not attacked | 3.43 | 0.59 | 68.66 | 10.71 | 15.12 |
| Surface attacked by HCl | 9.58 | 3.58 | 60.60 | 8.77 | 14.94 |
| Surface treated by the COREMIX-based gels | 8.65 | 1.91 | 62.81 | 11.07 | 13.42 |
| Surface treated by Aspigel 100E | 7.61 | 1.59 | 65.01 | 10.32 | 13.41 |

The chemical composition of the initial sample is characteristic of a SS surface. After the HCl treatment, the weight percentages in C and O increase while the Fe weight percentage strongly decreases as well as the one of Ni but not so importantly. The Cr weight percentage is approximately

constant (maybe a slight decrease can be seen). This is the mark of the formation of an oxide layer particularly enriched in Cr and even in Ni. After both decontamination treatments, the weight percentages in O and Cr decrease, while the detected amounts of Fe and Ni increase. Thus, a part of the Cr-enriched oxide layer is eliminated after the gel treatments, confirming their efficiency.

By comparing the two processes, Aspigel 100E induces a more important decrease of the O and increase of the Fe, while Ni is more present after the COREMIX-based gels. This is consistent with a better efficiency of the Aspigel 100E to eliminate the Cr and Ni enriched oxide layer.

#### 2.2.3.2 On moderately oxidized samples mimicking a spent fuel reprocessing vessel, prepared at NNL

- Preparation of the samples

The moderate oxidized samples were prepared at NNL [9]. 304L steel coupons (Figure 24 on the left – 32 mm diameter, 3 mm thick) were boiled (~122°C) for 10 days under reflux in a simulated spent fuel reprocessing liquor simulant. The composition of the simulant liquor is detailed in Table 6. These conditions were selected to mimic the conditions in the medium- and high-active evaporators at the Sellafield nuclear site, UK. Tests were conducted using a glass reaction vessel fitted with a condenser and a temperature controlled isomantle heater (Figure 24 on the right). The coupons were held in a vertical orientation within the glass vessel using a bespoke glass cradle. Coupons were removed after 10 days and allowed to air dry in the fume hood.

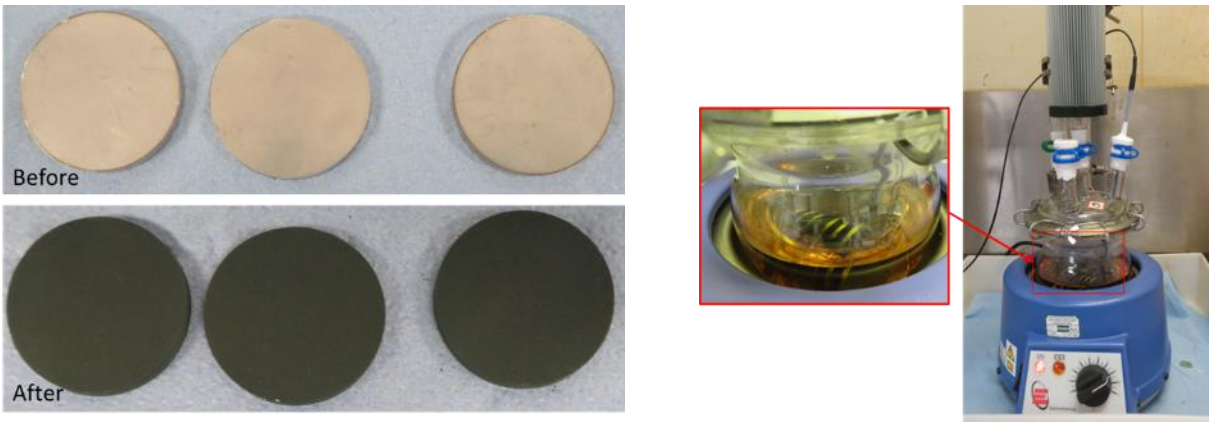


*Figure 24. 304L steel coupons before and after boiling in the spent fuel reprocessing liquor simulant.*

*Table 6. Spent fuel reprocessing liquor simulant*

| Element | Concentration (mol/teU) |
|---|---|
| N (from NH4) | 249.8642 |
| Na | 3.3256 |
| Al | 4.7808 |
| P | 6.3177 |
| K | 3.3256 |
| Cr | 10.2591 |
| Fe | 35.8121 |
| Ni | 6.9232 |
| Rb | 3.2056 |
| Sr | 7.3018 |
| Y | 3.7860 |
| Zr | 31.2946 |
| Mo | 24.5582 |
| Re for Tc | 5.0044 |

| | |
|---|---|
| Ru | 7.6652 |
| Rh | 1.7711 |
| Pd | 7.0967 |
| Te | 2.4356 |
| Cs | 15.0390 |
| Ba | 8.9837 |
| La | 6.8192 |
| Ce | 14.1824 |
| Pr | 5.8724 |
| Nd | 21.7380 |
| Sm | 4.1509 |
| Eu | 1.2901 |
| Gd | 25.4372 |
| V for Np | 1.1097 |

- Performances evaluation

The protocol described on Figure 18 was applied to evaluate the decontamination performances of the COREMIX-based gels. Experiments were also performed with the commercial Aspigel 100E. The Figure 25 shows some pictures of the experiments.

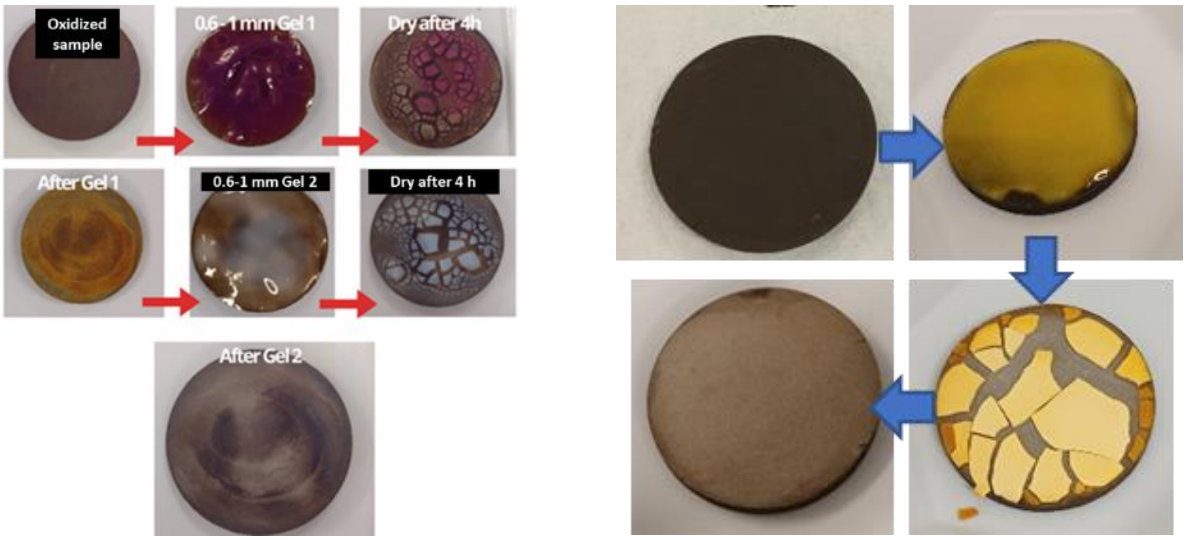


*Figure 25. Pictures of a decontamination operation of a moderately oxidized SS sample using the COREMIX-based gels (left) and the Aspigel 100E (right).*

The pink colour of the initially applied COREMIX-based gel (characteristic of the presence of permanganate ions) was lost after the drying, which is a mark of the oxidation reaction (Figure 25 on the left). After elimination of the solid residues, the sample presents an orange tint representative of iron oxides. Then, the second gel (containing oxalic acid) dissolved and removed the iron oxides. At the end of the process, an important part of the oxidized black surface was eliminated and a mass loss of 0.4 mg was measured, illustrating the COREMIX-based gels decontamination efficiency, even if some traces are still visible. The two gels was applied once and the experiment was referred to as “P1”. Another experiment, named “P2”, with two successive applications of the process was also performed and lead visually to a more important elimination of the black oxidized layer. This was confirmed by the increase of the mass loss (2.6 mg).

The Figure 25 on the right presents the results obtained with one application of Aspigel 100E. After drying, the yellow color in the solid residues is less intense, synonym of the reduction of the Ce(IV) and so the chemical reaction with the substrate. At the end of the process, all the black oxidized

layer was removed. A mass loss of 35.1 mg was determined, which is much greater than the mass loss obtained with the COREMIX-based gels.

The Figure 26 presents SEM images at different magnifications of the SS coupons before and after the decontamination experiments.

| | | |
|---|---|---|
| (i) Before contamination | 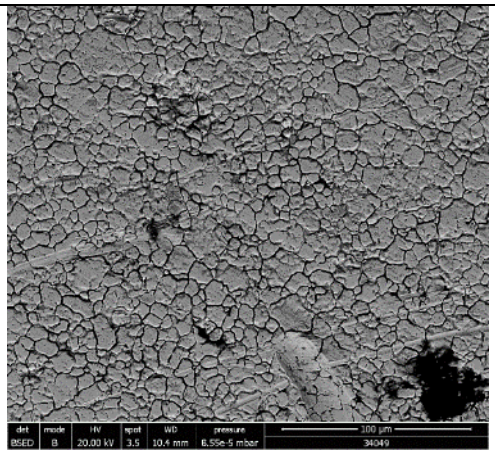 | 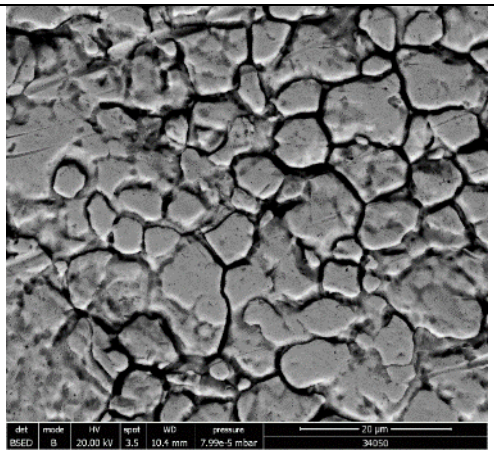 |
| (ii) After contamination and before decontamination | 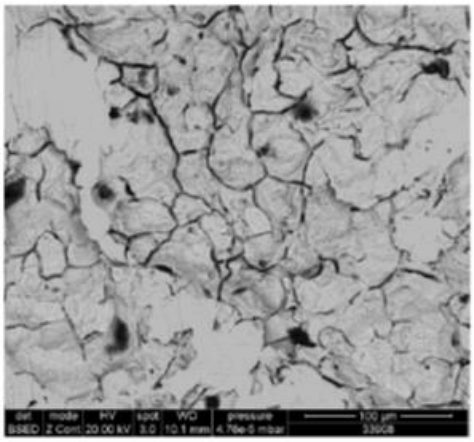 | 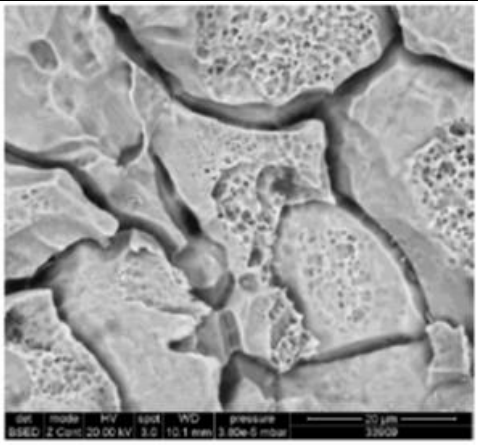 |
| (iii) After 1 treatment with COREMIX-Gel | 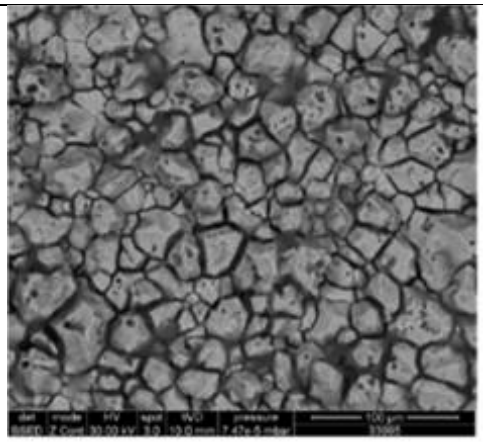 | 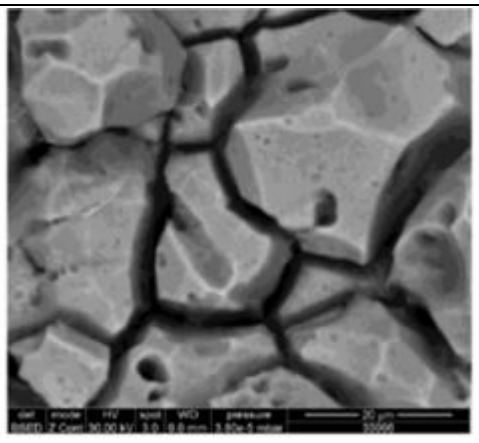 |

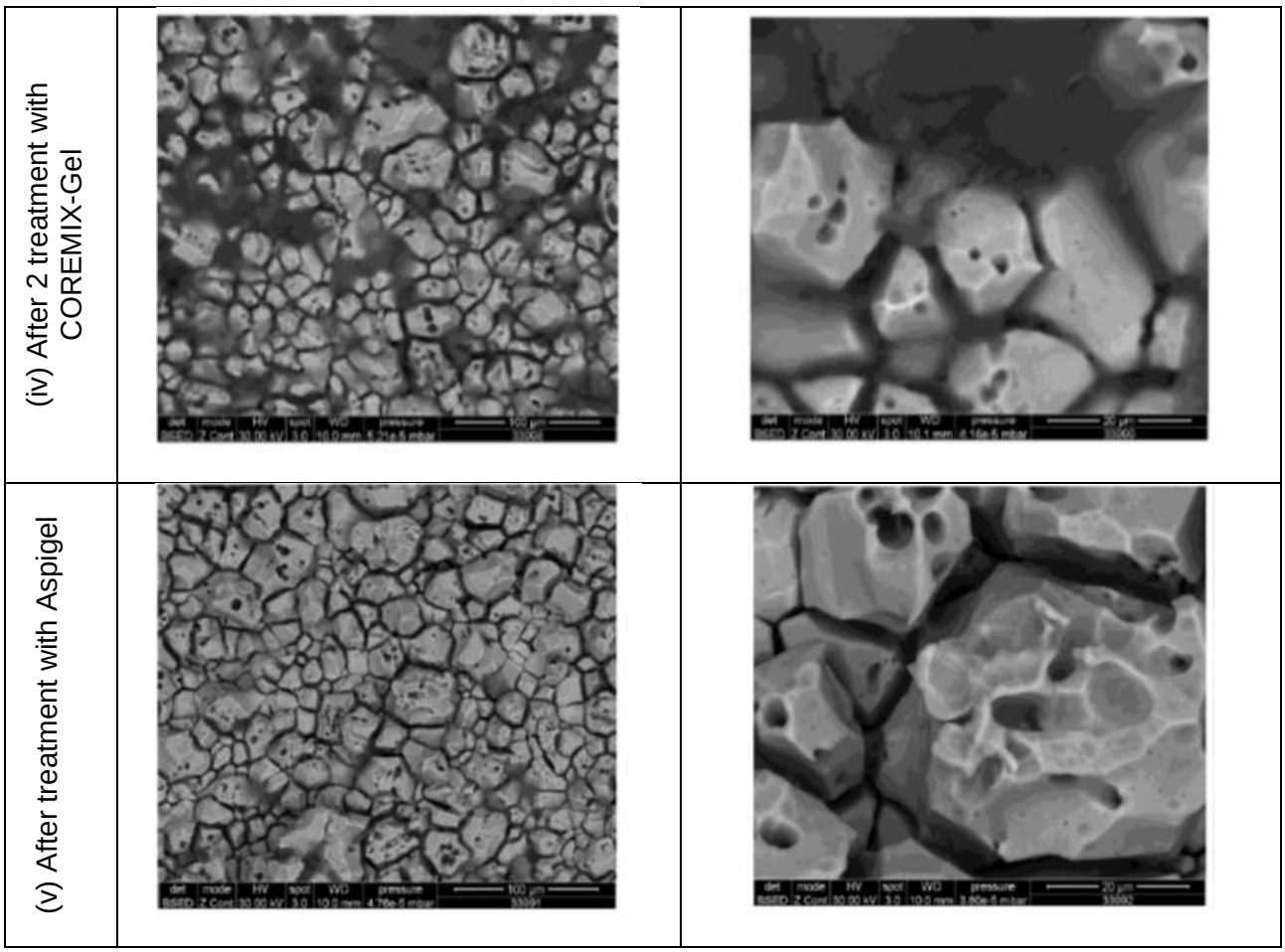


*Figure 26. SEM images at different magnifications of the (i) the initial SS sample (i) before and (ii) after contamination, (iii) the SS samples treated with one (center left), (iv) two applications (center right) of the COREMIX-based gels and (v) the SS sample treated with Aspigel 100E (bottom).*

The images of the substrate before application of the gels show the presence of the oxide layer, covering the asperities of the SS substrate. Images realized on the different samples after the three experiments (P1, P2 and Aspigel 100E) illustrate the elimination of this oxide layer. No significant differences are observed after the different treatments, even if some residual traces are still visually present after P1 and P2.

X-ray fluorescence and X-ray diffraction analyses were then performed on the different samples (Figure 27).

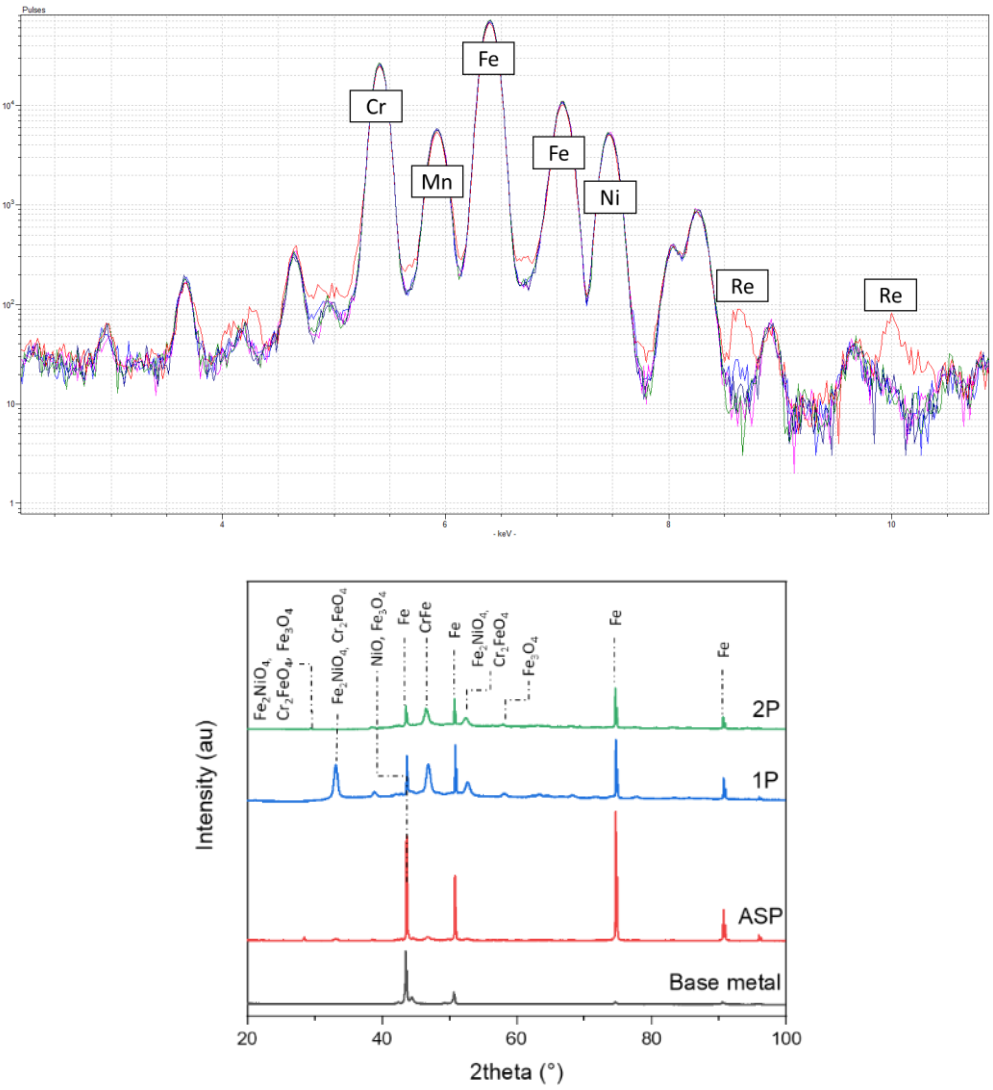


*Figure 27. X-ray fluorescence (up) and X-ray diffraction (bottom) analyses of different SS coupons. For X-ray fluorescence: initial sample is plotted in red, sample after Aspigel 100E treatment in green and samples after one and two applications of the COREMIX-based gels in blue and pink respectively.*

The peaks within the XRF spectra of the different samples mainly superimpose before and after the gel treatments with the identification of the metallic elements characteristics of the SS (Cr, Mn, Fe, Ni…). Interestingly, Re is identified at 8.5-8.6 keV and 10 keV on the XRF spectrum of the coupons before the gel treatment and not anymore after the decontamination operations, highlighting the process efficiency. Note that a slight peak characteristic of the Re is still identified on the sample treated with one application of the COREMIX-based gels, showing that this protocol is the less efficient.

Moreover, the X-ray diffractograms show that the sample treated with Aspigel 100E is close to the base metal, confirming the removal of the oxide layer. However, some remaining oxides peaks were still identified on the samples treated with the COREMIX-based gels. 1P has notably quite different oxide peaks, which reduce with the 2P process 2P. This is consistent with the visual observation of residual black traces after 1P, less important after 2P, and the XRF characterizations.

The solid residues of the gels were finally dissolved in HF and analysis by ICP-OES. Figure 28 presents the different masses of Cr, Ni and Fe determined in these residues. Note that, for the COREMIX-based gel process, all the masses (coming from the different gels) have been accumulated to illustrate the efficiency of the complete operation.

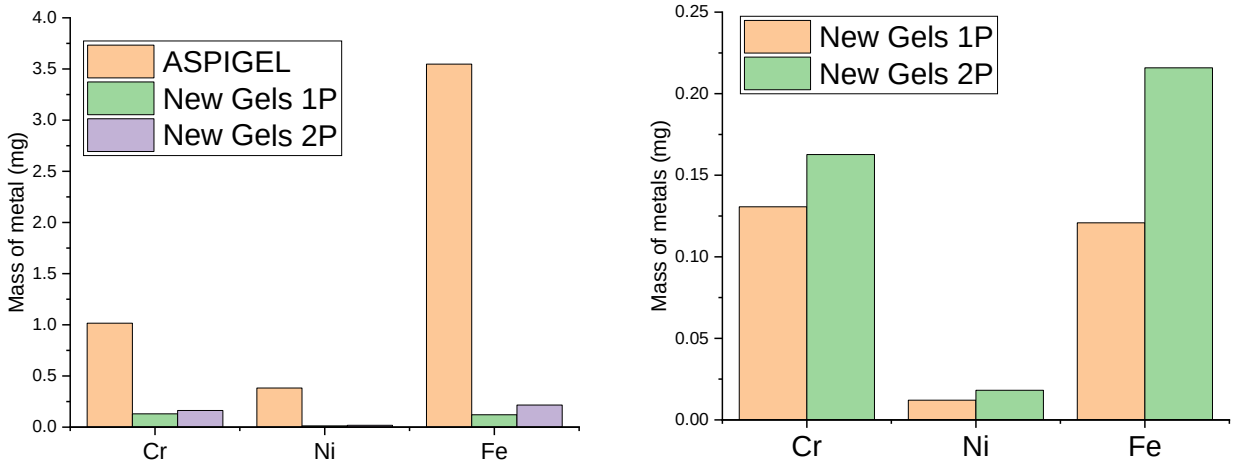


*Figure 28. Masses of metal in the solid residues after the gel decontamination tests: comparison between the three experiments on the left, and only the experiments using COREMIX-based gels on the right.*

These results are in accordance with the previous characterizations. Figure 28 shows that larger amounts of metals were analyzed in the final solid residues of the Aspigel 100E than in the two experiments with the COREMIX-based gels. This demonstrates that the Aspigel 100E is globally more efficient than the COREMIX-based gels. Moreover, Figure 28 also highlights the requirement to make successive applications of the gels in order to increase of the surface metal dissolved from the SS samples. The COREMIX-based gels (2P) eliminates 4,7 and 5,9 % of Ni and Fe respectively compared to the amounts eliminated with Aspigel 100E, and 15,7 % for Cr. Thus, the COREMIX-based gels are quite effective for to oxide the enriched-Cr layer and the limitation may come from the oxalic acid based gel.

To complete these data, the concentration in Re was determined in the different solutions after dissolution of the solid residues. Indeed, Re is present in the oxidized layer of the samples and not in the pristine metal composition. Thus, a large amount of Re was measured in the residues of Aspigel 100E, highlighting its efficiency. Then, Re was also detected in the oxidative gel (containing $KMnO_4$ and $HNO_3$), but not in the oxalic acid based gel. In this way, it could be assumed that most part of the Re is present in the Cr enriched oxide layer.

#### 2.2.3.3 On strongly oxidized samples simulating a steam generator corrosion, prepared at SORC

- Preparation of the samples

The samples were synthesized by SORC (Hungary) as described above (contacting SS coupons with a flow of water vapour at 800°C during 8 hours).

- Performances evaluation

The protocol outlined in Figure 18 was applied on a strongly oxidized SS coupons and pictures of the different steps are illustrated in Figure 29.


*Figure 29. Decontamination of strongly oxidized SS samples by the COREMIX-based gels.*

Visual observations showed that the COREMIXC-based gels were not very efficient on strongly oxidized samples, contrary to results obtained with liquid solution [1]. Indeed, using the liquid solution induces a larger volume of decontamination reagents and an infinite contact with the substrate, while vacuumable gels are, by definition, subjected to drying and evaporation of the decontamination solution, which limits the chemical reactions. Note that, due to this visual poor efficiency, no effort were done on further metal characterization.

### 2.2.4 Conclusion

A new two-step decontamination gel process has been developed based on the COREMIX process. An initial gel, containing 15 mmol.L-1 of $KMnO_4$ and 3 mmol.L-1 of $HNO_3$ with 9 %wt of silica NPs as a viscosing agent, was used to oxidize an enriched Cr layer. After drying, a second gel, containing 18.5 mmol.$L^{-1}$ of oxalic acid and 9 %wt of silica NPs as a viscosing agent, was applied to dissolve iron phases. This new process was shown to be efficient to decontaminate slightly or moderate oxidized SS surfaces, but they were still less effective than the commercial Aspigel 100E containing nitric acid and Ce(IV). However, these new gels may be utilised as an alternative to Aspigel 100E, notably in situation where Ce(IV) cannot be used (e.g. not compatible with available secondary waste routes) or if soft decontamination operations are required, i.e. only very slight surface removal required to not deeply corrode the surface.

Finally, all the tested vacuumable gels have shown very limited efficiencies on strongly oxidized substrates with multi-layered corrosion of some microns. At this point, this may appear as a limitation of the process. Indeed, the volume of decontamination solution at the contact of the contaminated substrate is low compared to bulk chemical immersion e.g., using a liquid bath for example. Moreover, the evaporation during drying hinders the chemical reaction. Consequently, even if the vacuumable gel process presents clear advantages in term of application and secondary waste management, the principle of the process restricts the efficiency to thin corrosion layer. Further studies could be performed improve this by multiplying successive applications, decrease the drying time or make experiment at higher temperatures to increase the reaction kinetic.

# 3 New application processes to use vacuumable gels for the decontamination of small objects with complex geometries

As described above, the vacuumable gels are particularly adaptable to be sprayed on large and plane surfaces, such as the walls of hot cells for example. However, a large part of the metallic waste are small objects, such as pipes, valves or pump, having sometimes complex geometries and surfaces hardly accessible for the gel if it is applied by spraying. This consequently limits the use of

the decontamination gel presented in this report. For that purpose, two innovative ways to use decontamination gels have been studied:

- Use the gel as a bath, allowing to dip the contaminated items and leave a thin layer of gel on the whole surface. In this way, unlike a liquid bath, the decontamination occurs outside the bath, avoiding its contamination. The gel bath can then be used for other decontamination operations.

- Incorporate ferromagnetic particles in the gel formulations to spread them using a magnet, and thus possibly on inaccessible surfaces.

## 3.1 Use a vacuumable gel as a bath to dip small objects with complex geometries

Few years ago, a solution using thermo-responsive gels in form of bath rather than by spraying was proposed by Castellani et al. [10] to treat small items with complex geometries. The contaminated material is immersed in a cold bath of liquid gel, which ensures a perfect coating even if the object's geometry is complex. If the object is cold, the gel remains liquid and flows over the surfaces. If the piece is heated prior to immersion however, the gel's viscosity increases upon contact and remains attached to the surface. However, such formulations includes thermo-responsive organic compounds, which are not well suited for nuclear applications due to their weak irradiation resistance.

In this way to avoid the presence of organic compounds in the secondary waste induced by the decontamination operation, we decided to evaluate the possibility to directly use vacuumable gels "as it" as a bath.

### 3.1.1 Proof of concept on model gels "Alumina-water": formulation requirement

The proof of concept of the "bath process" was first demonstrated on model gels. These gels consisted in a dispersion of alumina particles (Aeroxide Alu C, Evonik Industries) in water. Alumina particles were used because alumina-based gels present simple rheological properties compared to silica-based gels with no thixotropy [11].

First, the influence of the amount of alumina particles in the gel was tested. For that, three gels were formulated by mixing alumina particles in water with different weight percentage in alumina: 20%wt, 25%wt and 33%wt. Then, samples of 316L SS were dipped in the different gels for 1 second. The dipping experiments were performed using an Ossila Dip-Coater device. The deposited gel mass was evaluated by weighting the coupons before and after the dip. The Figure 30 on the left presents the evolution of the deposited mass of gel as a function of the alumina weight percentage.

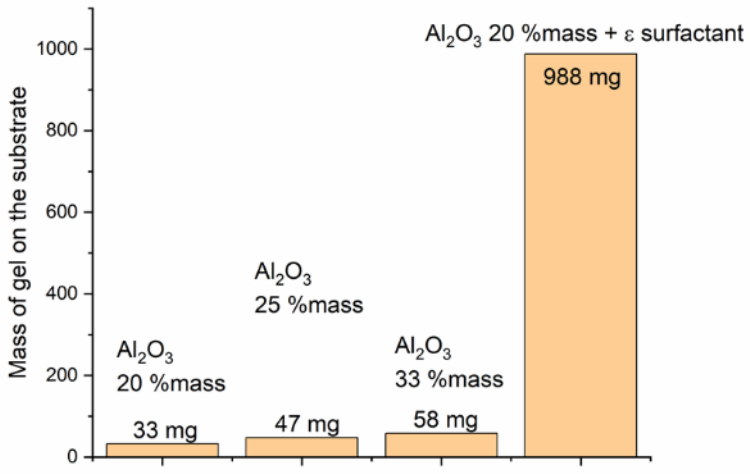


*Figure 30. Mass of gel deposited on a SS substrate dipped in different gel formulations (left) and pictures of layers of 20 %wt alumina-based gels without (center) and with a small amount of surfactant (right) on a SS substrate after dipping.*

Figure 30 shows the coupon before and after immersion in the bath of a gel containing 20%wt of alumina. The gel layer was extremely thin and almost invisible. This observation was similar whatever the amount of alumina particles in the gel formulation (only a very slight increase of the deposited mass of gel). The gels did not adhere very much to the SS substrate and slip on the coupon when it is removed from the bath.

To improve the wettability of the SS surface by the alumina-based gel, a small amount of surfactant was added to the gel containing 20 %wt in alumina. The used surfactant was a three tri-block copolymer poly(ethylene oxide)$_{14}$-poly(propylene oxide)$_{31}$-poly(ethylene oxide)$_{14}$ whose commercial name is Pluronic PE6200 (BASF) [11]. After a dipping experiment, the gel containing the surfactant left a thin layer on the coupon, as observed in Figure 30. Moreover, the mass of gel deposited on the SS coupons significantly increased with a factor around 30. This phenomenon could be explained by the better wettability of the SS coupon by the liquid solution in presence of a surfactant, allowing a better adhesion of the gel on the surface, as well as better viscoelastic properties allowing the maintain of a gel layer on a vertical surface.

Comparing these results, the presence of the surfactant in the gel formulation seemed to be necessary to have a significant gel coating on a SS surface. We then studied the influence of the surfactant PE6200 concentration on the gel properties. For that, different amount of PE6200, between 0.001 %wt and 18 %wt, have been added to a gel containing 20 %wt of alumina particles.

First, the influence of the presence of surfactant of the gel spreading on a SS surface was studied. For that, drops of equal volumes of the different gels were deposited on SS coupons and pictures were taken using a using a Tracker automatic drop tensiometer (Teclis Scientific). The contact angle was directly measured on the pictures. Figure 31 illustrates the observed evolution of the contact angle with the increase of the surfactant concentration. Moreover, the yield stress of the gels were determined by rheological analyses [11]. The yield stress represents the stress to apply to make the gel flows. An important yield stress makes the gel “solid like” although gels with a low yield stress behave more like liquids. The Figure 31 on the right shows how the surfactant concentration affects the yield stress of the gels.

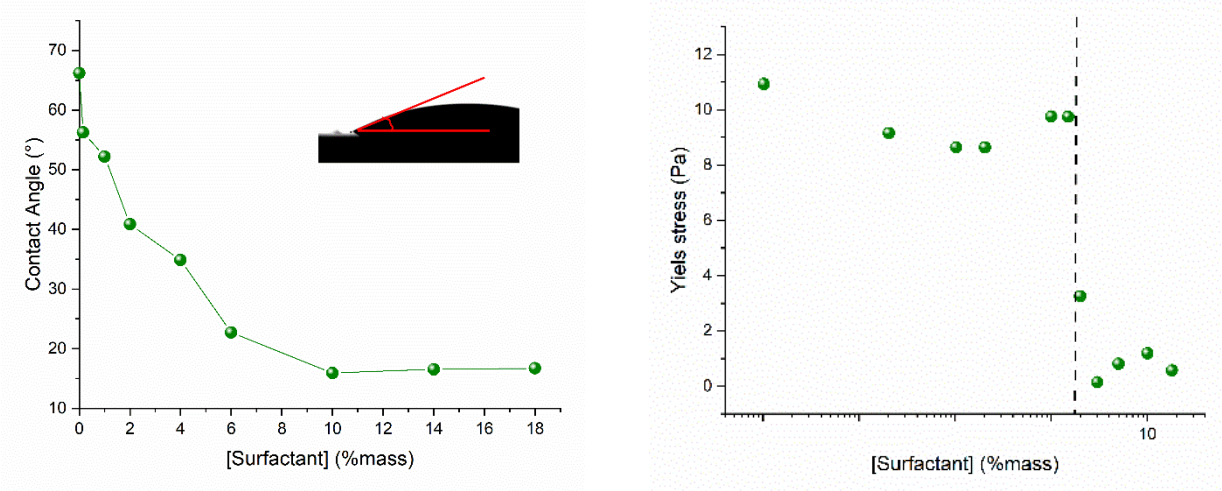


*Figure 31. Influence of the surfactant concentration on the contact angle of a 20 %wt alumina gel with a SS surface (left) and on the gel yield stress (right).*

Adding surfactant to the gel formulation modified the gel-substrate interaction but also the internal structure of the gel. Indeed a larger amount of surfactant lead to a better spreading of the gel on a SS surface. However, from a surfactant concentration of around 2 %wt, the yield stress of the gel drastically dropped. These both evolutions influenced the gel deposition. Figure 32 shows the mass

of gel deposited on SS coupons after their dipping in bath of gels containing 20 %wt in alulmina and different concentration in surfactant. The thickness of the deposited gel layers were measured using a specific toothed tool (see Figure 32 on the right).

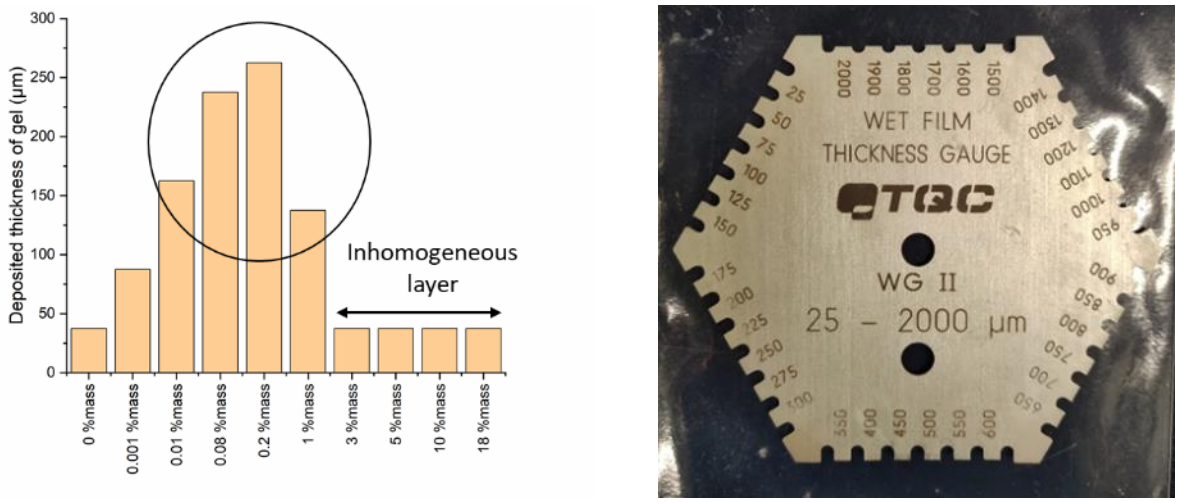


*Figure 32. Influence of the surfactant concentration on the deposited gel thickness (left) measured using a specific toothed tool (right).*

For low surfactant concentrations, the gel deposited thickness increased until reaching a plateau. Indeed, the gel better spread on the SS substrate with the increase of the surfactant concentration, while the gel yield stress was not impacted. Thus, the gels were able to adhere to the surface and did not flow. Then, for surfactant concentrations higher than 1 %wt, the gel thickness where found to decrease until no gel is no more deposited (or unless under thin and inhomogeneous layers). From this point, even if the gels could wet well the SS substrate, they lost their yield stresses and consequently their texture and could not form smooth and cohesive layers anymore.

Finally, we have first performed studies on model gels to highlight the physicochemical relationship between gel components and their influence on the process. By coupling rheology and contact angle measurements, we have demonstrated that the presence of surfactant is a key parameter for the gel to wet the surface and cover at best the metallic pieces. However, the surfactant concentration was found to be critical and a maximum identified not to overpass to avoid any disturbance of the gel and thus maintain the surface covering properties.

### 3.1.2 Efficiency of a commercial gel to be used as a bath

The commercial Aspigel 100E was tested via the bath “dipping process”. Figure 33 illustrates the different experimental steps.

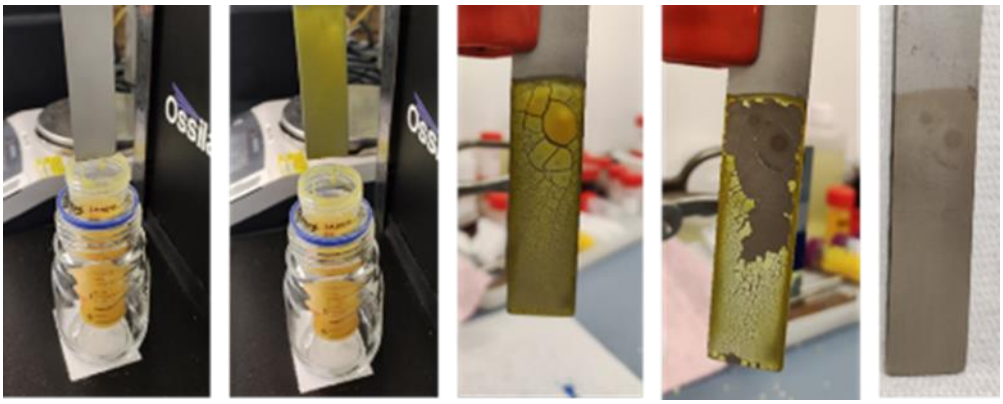

*Figure 33. Deposition and drying of an Aspigel 100E layer on a 316L SS coupon using a “dipping process”.*

Before dipping a 316L SS coupons, the gel needed to be gently sheared to decrease its viscosity until obtaining a creamy texture. Indeed, Aspigel 100E is a stiff silica-based gel, thus this step was crucial. The 316L SS samples were dipped and the deposition of a smooth layer of gel was observed. Because the formulation of the range of Aspigel (commercialized by the FEVDI Company) are derived from a CEA patent [12], they contain a small amount of surfactant, whose nature depends on the decontamination solution, to adjust their rheological properties. As previously shown, this makes such gels efficient to be used in a dipping process. After drying and elimination of the solid residues, the dissolved metal thickness was estimated at 0.3 µm, which is consistent with the deposition of a millimeter gel layer with other processes.

In this way, we have demonstrated that the Aspigel 100E can be used in a dipping process, which is promising for the decontamination of small metallic objects having a complex geometry and surfaces hardly accessible.

## 3.2 Application of decontamination gels on hardly accessible surfaces: presentation of a new application process

Another process using decontamination gels was patented [5] and studied during the PREDIS project. For that purpose, the formulation of vacuumable gels was modified to be applied on hardly accessible surfaces using a magnet.

### 3.2.1 Application of decontamination gels on hardly accessible surfaces: presentation of a new application process using a magnet

This new technology aims to apply decontamination gels on hardly accessible surfaces without spraying or manual depositing. For that purpose, ferromagnetic particles were added to gel formulations. In this way, the gel acquires a “magnetic” response. Indeed, by moving a magnet close to the gel, even through a surface, the gel can be spread thanks to the presence of ferromagnetic particles and its rheological properties. Then, after decontamination and drying, secondary solid waste are produced, as for vacuumable gels, and contain the ferromagnetic particles. Thus, they can be recovered by attraction with a magnet. In this way, we are able to formulate of new range of decontamination gels, called “magnetic gels”, which can be used on hardly accessible surfaces, such as the internal surface of a pipe for example. Figure 34 schematically illustrates this new application process.

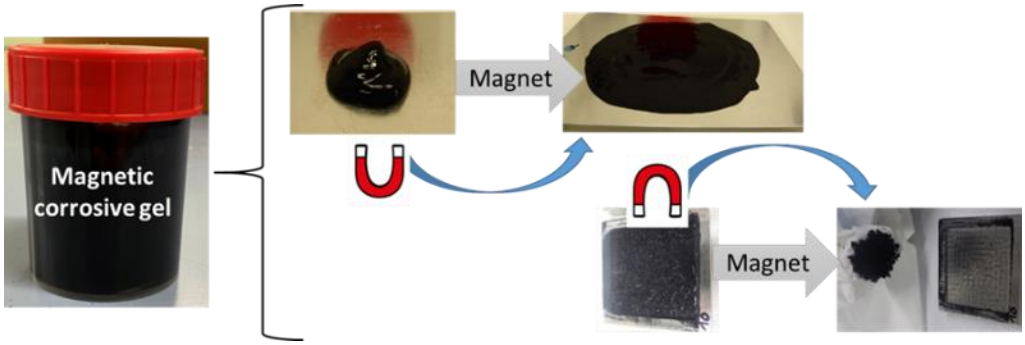


*Figure 34. Schematic description of the application of a magnetic gel and the recovering of the solid residues after drying.*

### 3.2.2 Proof of concept on model gels “Alumina-water”

First experiments were tested on model gels consisting in a dispersion of alumina particles (Aeroxide Alu C, Evonik Industries) in water. Alumina particles were used because alumina-based gels present simple rheological properties compared to silica-based gels, notably with no thixotropy [11]. Thus, ferromagnetic particles ($Fe_3O_4$, Iron (II, III) oxide powder, Sigma-Aldrich) were mixed either with only water or with alumina particles and water. The formulations are given in Table 7.

*Table 7. Model gels used for the "magnetic gel" proof of concept.*

| Gel number | Water [%wt] | Alumina particles [%wt] | $Fe_3O_4$ particles [%wt] | Total weight percentage of solid phase [%wt] |
|---|---|---|---|---|
| Gel_1 | 50 | 0 | 50 | 50 |
| Gel_2 | 66.7 | 0 | 33.3 | 33.3 |
| Gel_3 | 41.5 | 37.7 | 20.8 | 58.5 |

Gel_1 and Gel_2 were formulated only with high amounts of $Fe_3O_4$ particles dispersed in water. This lead to two viscous fluids, Gel_1 being more viscous than Gel_2 because having a larger amount of solid particles. The spreading properties of the gel were evaluated by using a commercial magnet (N829 from Eclipse Magnetics). After gel deposition, the magnet was placed on the opposing face of the targeted metal surface and slowly moved unidirectionally. Figure 35 shows some pictures of the process.

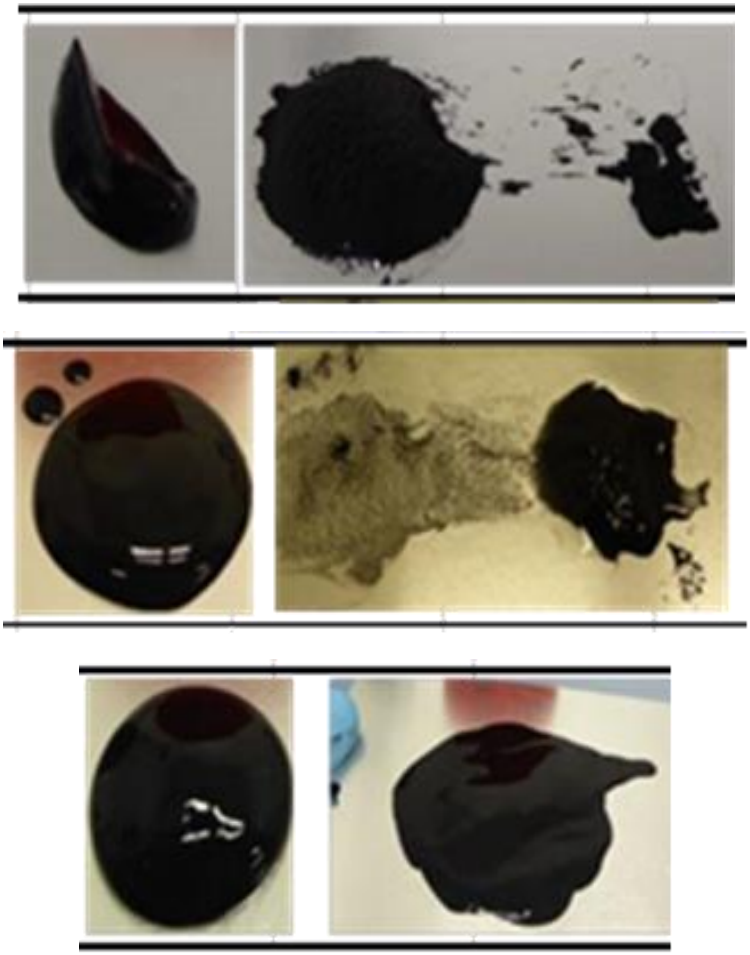

*Figure 35. Pictures of the Gel_1 (top), Gel_2 (center) and Gel 3 (bottom): knobs manually deposited on a surface (left picture) and spreading properties using a magnet (performed from left to right).*

Inhomogeneous coverage was observed when Gel_1 and Gel_2 were tested. For this reason, alumina particles were added to the formulation of Gel_3, which improved the rheological features and make the gel able to adhere to the surface. These tests showed there was a necessity to have

both ferromagnetic particles and a viscosing agent to formulate a magnetic gel. Figure 36 shows the process of applying a millimeter thick layer of Gel_3, allowing it to dry and the resulting magnetic non-powdery solid residue.

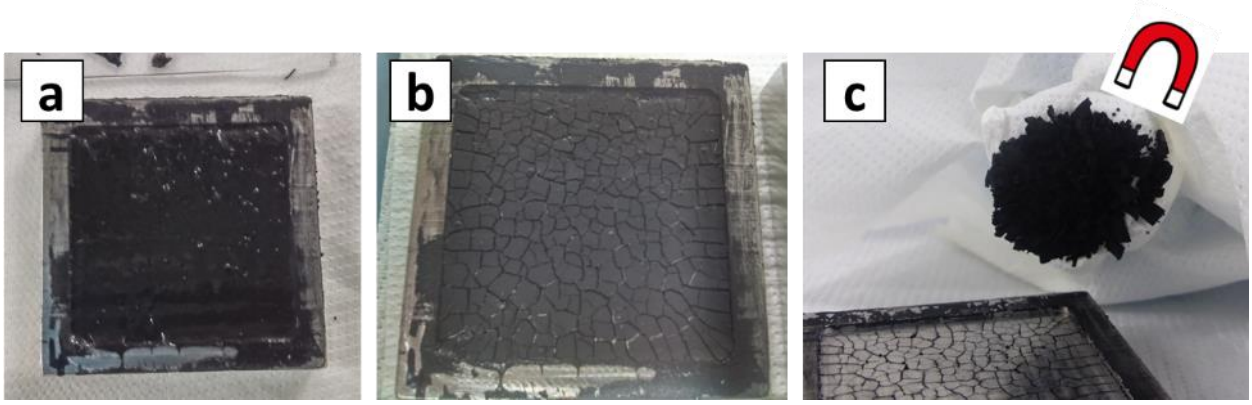


*Figure 36. Millimeter layer of Gel_3 (left), formation of solid residues after drying (center) and attraction of the solid residues by a magnet (right).*

Successful removal with a magnet was achieved, thus no necessity to brush or vacuum clean the surface and a promising feature for the decontamination of hardly accessible surfaces. Note: small volume residual solids did remain attached on the surface [13]. These residues were finally removed using a wet swipe to make the surface perfectly clean.

Finally, the principle of the "magnetic gel" process was demonstrated on a simple and model gel by coupling the presence of ferromagnetic particles and viscosing agent. Further studies have been then performed to evaluate the possibility to tune the formulation of a commercial gel able to decontaminate SS surfaces.

### 3.2.3 Formulation modification of a commercial gel to be used as a magnetic gel

The formulation of the commercial gel Aspigel 100E was modified by adding ferromagnetic particles (Iron (II, III) oxide powder, Sigma-Aldrich) at different concentrations (5, 8.5 and 13 %wt). They are referred to as Aspigel_x with x the weight percentage in $Fe_3O_4$. The magnetic gels were obtained by gently mixing an adapted amount of $Fe_3O_4$ particles with the Aspigel 100E. For that, the gel was manually mixed using a plastic spatula until obtaining a creamy like texture. The $Fe_3O_4$ particles were then added and the gel was homogenized to well disperse the particles. Finally, the gel was let to rest for 1 day before being used.

#### 3.2.3.1 Influence of the ferromagnetic particles concentration on the displacement of the gel using a magnet

- Rheological behavior

To better understand the behavior of the magnetic gels having different weight percentage in $Fe_3O_4$ (5, 8.5 and 13 %wt) and anticipate their spreading properties with a magnet, their rheological properties were analyzed using a TA instruments Discovery Hybrid Rheometer (DHR 1). For that, a small shearing of 1 $s^{-1}$ was applied for 1 minute to simulate a shearing of the gel equivalent to a manual deposition on a surface. During this shearing phase, the gel viscosity decreases, notably because the silica particles network (allowing the "gel-state") is broken and silica particles follow the shearing flow [14]. Thus, the gel was still a shear-thinning fluid even after the addition of the ferromagnetic particles. This shearing was immediately decreased to a very low value (0.015 $s^{-1}$) to simulate the gel at rest directly after the manual deposition, and the viscosity was followed with time for 45 minutes. The evolution of the viscosities with time are shown Figure 37.

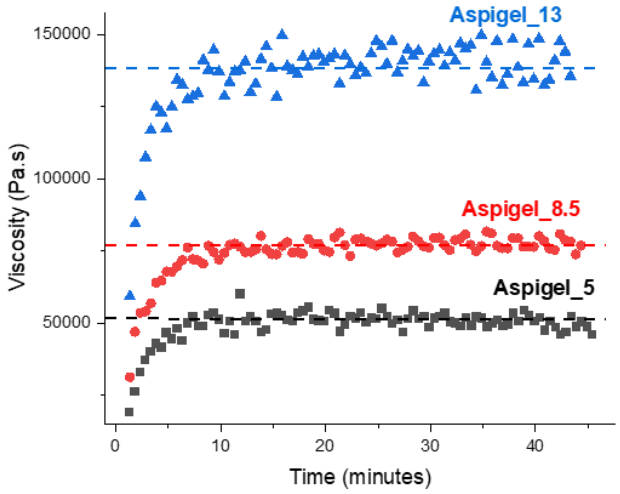


*Figure 37. Viscosity recovery with time after a 1 minute shearing step at 1 $s^{-1}$ for the Aspigel_5 (black squares), Aspigel_8.5 (red circles) and Aspigel_13 (blue triangles).*

For the three gels, a strong increase of the viscosity was observed during the first minutes, before a plateau was reached. Indeed, silica-based colloidal gels are thixotropic fluids and, during the period following the shearing, the silica particles re-organizes themself to recreate a viscous network and strength the suspension into a gel again. As the magnetite particles concentration in the gel formulation was increased, higher viscosity values were measured, and consequently the global viscosity of the gel. Thus, an increased solid volume lead to a more compact gel-state [15].

- Spreading tests on a stainless steel substrate using a magnet

To evaluate the gel spreading properties of the gel, drops of gel (with a known mass) were first deposited on the SS coupons (Figure 38a). Then, a magnet (N829 from Eclipse Magnetics) was placed on the opposing face of the coupons and slowly moved in a circular motion. Thanks to the presence of the ferromagnetic particles, the gel spread on the coupon (Figure 38b) and this operation was performed until the gels no longer moved at the passing of the magnet. At this point, the viscosity and the adherence of the gel to the substrate overpassed its magnetic response.

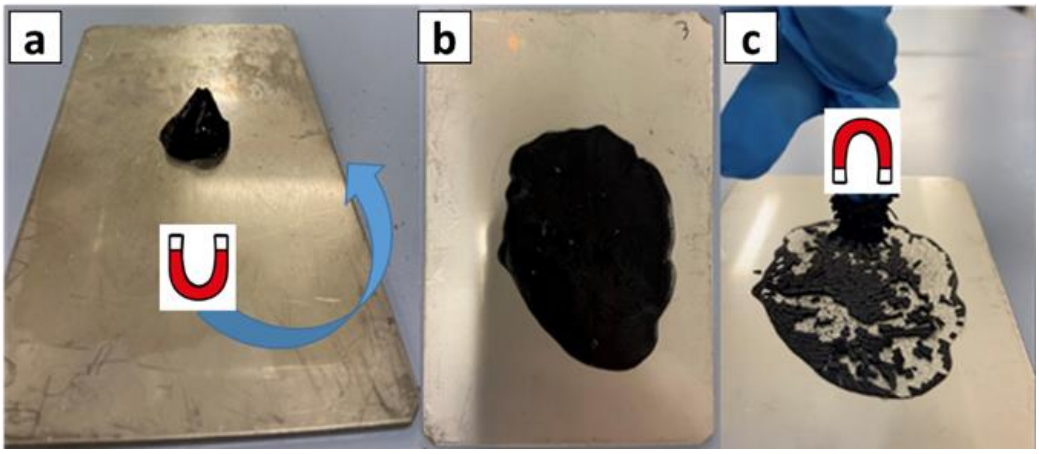


*Figure 38. Different steps of a SS sample decontamination using a magnetic gel: (a-b) Manual deposition of a drop of gel and spreading of the gel using a magnet, (c) Recovering of the solid residues obtained after drying using a magnet.*

After spreading, a picture of the gel layer was taken and its area was determined using the ImageJ software. This data were then used to calculate the gel spreading property (in $cm^2.g^{-1}$, see Table 8).

Moreover, with the calculation of the gel density (obtained directly from the densities of the Aspigel 100E and the magnetite particles), an average gel thickness was calculated using Equation 5.

Equation 5 $$Average\ gel\ thickness = \frac{m}{S \times d}$$

Where m the deposited mass of gel, S the surface determined using by the ImageJ software and d the gel density value (depending on the amount of ferromagnetic particles).

The different gel thickness values are reported in the Table 8 and the influence of the ferromagnetic particles amount in the gels on their deposited thickness is shown on Figure 39. Gels with the greater amount of ferromagnetic particles had the weakest spreading properties. Particularly, for a similar mass of deposited gel, the area of the gel layer obtained using a magnet decreases and, as a result, the gel deposited thickness is higher. Indeed, although the magnetic response should be higher due to the presence of more ferromagnetic particles, the viscosity of the gel increased significantly, as shown Figure 37, which has a strong impact on the gel displacement possibility. There is consequently a direct relationship between the gels magnetic sensibility, their rheological properties and the gel deposited thickness; and only a small amount of ferromagnetic particles is enough to spread the gel to a satisfying thickness.

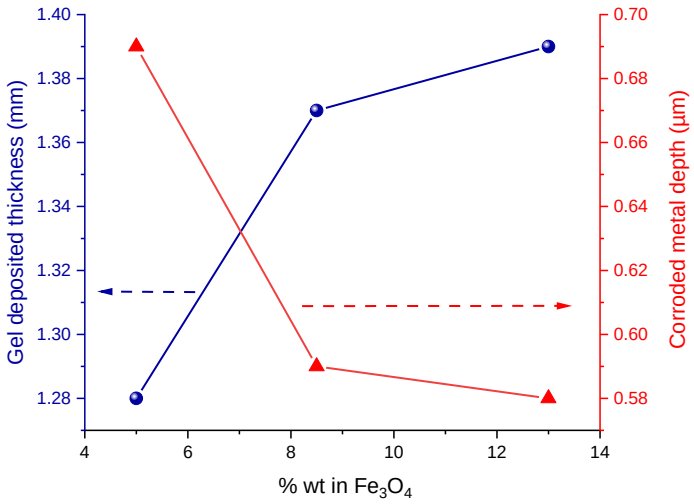


*Figure 39. Influence of the amount of ferromagnetic particles added in the geld on their spreading properties and corrosion efficiencies.*

*Table 8. Summary of the data determined from the different experiments using the Aspigel_x.*

| Gel | Calculated density | Aging | Gel spreading ($cm^2 \cdot g^{-1}$) | Gel deposited thickness (mm) | Corroded metal depth (µm) | Percentage of recovered flakes (%) |
|---|---|---|---|---|---|---|
| Aspigel_5 | 1.35 | / | 5.90 +/- 0.39 | 1,28 +/- 0.08 | 0.69 +/- 0.08 | 91.7 +/- 0.8 |
| | | 1 week | 8.51 +/- 0.39 | 0.88 +/- 0.04 | 0.35 +/- 0.02 | 95.5 +/- 0.4 |
| | | 2 weeks | 8.80 +/- 0.42 | 0.85 +/- 0.04 | 0.28 +/- 0.02 | 91.6 +/- 0.7 |
| | | 3 weeks | 9.36 +/- 0.40 | 0.80 +/- 0.03 | 0.21 +/- 0.02 | 90.0 +/- 0.9 |
| Aspigel_8.5 | 1.39 | / | 5.38 +/- 0.37 | 1,37 +/- 0.08 | 0.59 +/- 0.04 | 92.6 +/- 0.4 |

| | | | | | | |
|---|---|---|---|---|---|---|
| | | 1 week | 6.16 +/- 0.22 | 1.18 +/- 0.04 | 0.36 +/- 0.02 | 91.8 +/- 0.8 |
| | | 2 weeks | 6.51 +/- 0.21 | 1.11 +/- 0.04 | 0.27 +/- 0.02 | 96.8 +/- 0.5 |
| | | 3 weeks | 7.06 +/- 0.27 | 1.03 +/6 0.04 | 0.20 +/- 0.01 | 95.6 +/- 0.3 |
| Aspigel_13 | 1.44 | / | 5.00 +/- 0.16 | 1,39 +/- 0.04 | 0.58 +/- 0.02 | 91.5 +/- 0.8 |

- Secondary solid waste recovery using a magnet and evaluation of the SS corroded thickness

After gel drying, millimeter solid residues were obtained. Thanks to the presence of the ferromagnetic particles in these residues, they can be easily removed by attraction with a magnet (N829 from Eclipse Magnetics), as shown Figure 38c. Pictures were taken before and after the solid waste recovery and were analyzed by the ImageJ software. First, no specific influence of the gel formulation was observed on their size and shape. It seems that the drying step and the formation of the solid residues is controlled rather by the presence of the silica particles initially present in the gel than by the ferromagnetic particles. Moreover, the differences in the gel thicknesses are not significant enough to observe variation in the solid size as it could be expected [13]. Then, the large majority of the solid residues (more than 90 % for each formulation, see Table 8) can be recovered with the magnet. The remaining residues mainly come from very thin gel thicknesses on the edge of the gel layer, leading to smaller agglomerates more adhered to the surface [13]. These residual solids can be finally eliminated using a wet wipe or by a slight washing with water and ethanol, and the SS substrate was finally weighted to determine the mass lost and consequently the SS corrosion depth using Equation 1. The evolution of the dissolved SS depth as a function of the amount ferromagnetic particles in the gel is shown Figure 39.

First, note that the determined depths of few tens of microns are of the same order of magnitude than the one obtained with the pristine Aspigel 100E without ferromagnetic particles (see Figure 39 and Table 8). Then, there is a significant influence of the presence of ferromagnetic particles on the efficiency of the gel. Indeed, while increasing the ferromagnetic particles concentration leads to larger layer thicknesses, the corrosion efficiency of the SS surface after gel drying decreases. However, a thicker gel layer was expected to induce a larger decontamination solution volume at the surface of the SS coupon and consequently a longer chemical reaction and a deeper corrosion, but the opposite was observed. The presence of too much ferromagnetic particles in the gel formulation had negative effects on both the spreading properties of the gels using a magnet and also their decontamination efficiency. This latter observation may be explained by a chemical evolution of the decontamination solution in presence of the ferromagnetic particles. To validate this hypothesis, 5 g of $Fe_3O_4$ particles were dispersed in different batches of 50 mL of a FEVDIRAD liquid solution. This solution, commercialized by the FEVDI Company, has the same chemical composition that the decontamination solution of the Aspigel 100E, i.e. $HNO_3$ and Ce(IV). After different contact times, solutions were filtered and analyzed by ICP to determine the concentration in ionic iron coming from the dissolution of $Fe_3O_4$. As observed on Figure 40, the amount of ionic iron in solution increases with the contact time between the particles and the solution.

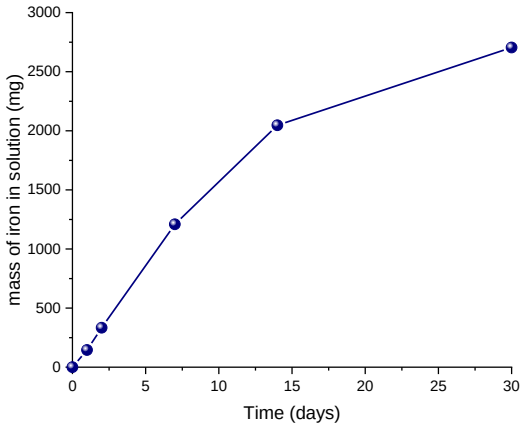


*Figure 40. Evolution with time of ionic iron in a FEVDIRAD solution, containing $HNO_3$ and Ce(IV), in contact with $Fe_3O_4$ particles.*

These results confirmed that there is a chemical reaction between $Fe_3O_4$ and the decontamination solution, leading to a dissolution of the particles and an increase of the ionic ion amount in solution. The increase is relatively linear until approximately 7 days and slows down for longer contact time, reaching an estimated dissolution around 74 % of the particles mass.

After decontamination, the different substrates were washed with water and ethanol. A dark coloration of the SS appeared at the end of the process. X-ray fluorescence and X-ray diffraction analyses were performed on the different samples (Figure 41).

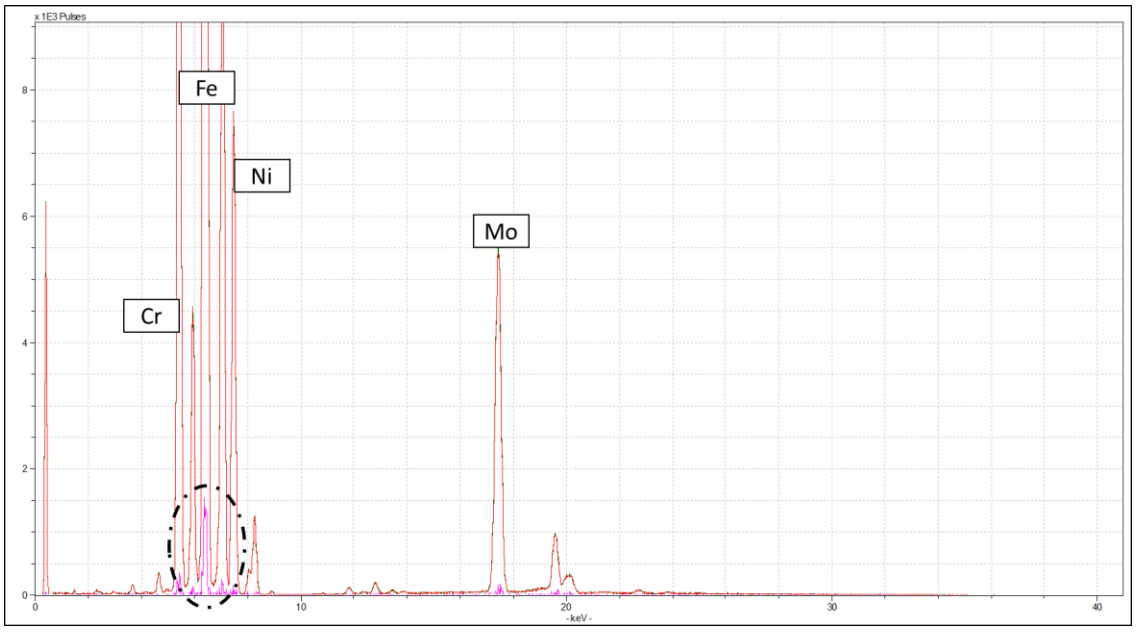

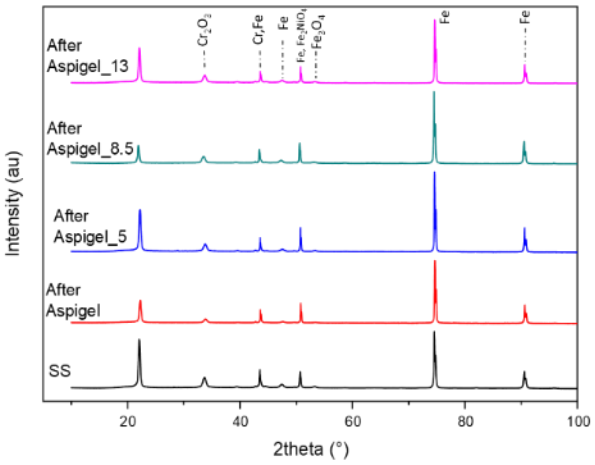


*Figure 41. X-ray fluorescence (top) and X-ray diffraction (bottom) analyses of different SS coupons treated using magnetic gels. For X-ray fluorescence: initial sample is plotted in red and sample treated by Aspigel_13, as an example, in green. As data almost superimposed, the pink plot corresponds to the difference between both spectra.*

The initial SS substrate was mainly composed of Fe, Ni, Cr and Mo, as illustrated by its XRF analysis. Then, the difference between the XRF spectra of the SS substrate before and after magnetic gel treatment shows a decrease of the amount of Fe, which could be characteristic of the formation of a thin oxide layer and consistent with the visual color variation. However, the X-ray diffractograms present no significant differences before and after the different Aspigel_x treatment and the oxide layer formed by the process was not detectable by XRD. Thus, we can reasonably conclude that is layer is certainly very thin. Finally, there was no difference between the surface treated with the Aspigel_100E or with the different magnetic gels, illustrating that the presence of ferromagnetic particles did not impact the mechanism decontamination.

#### 3.2.3.2 Aging of the magnetic gels and influence on their spreading and decontamination properties

As it was shown that the ferromagnetic particles react with the decontamination solution of the Aspigel 100E, the influence of the aging on the rheological, spreading and decontamination properties was studied.

- Evolution of the rheological properties with time

The rheological analysis protocol previously described was performed on the 3 magnetic gels at different aging times (1, 2 and 3 weeks). For that, a shear rate of 1 $s^{-1}$ was applied for 1 minute and then immediately decreased to a very low value (0.015 $s^{-1}$). The viscosity was followed with time for 45 minutes to reach a plateau. The Figure 42 presents the evolution with time of the plateau viscosity values of the 3 magnetic gels.

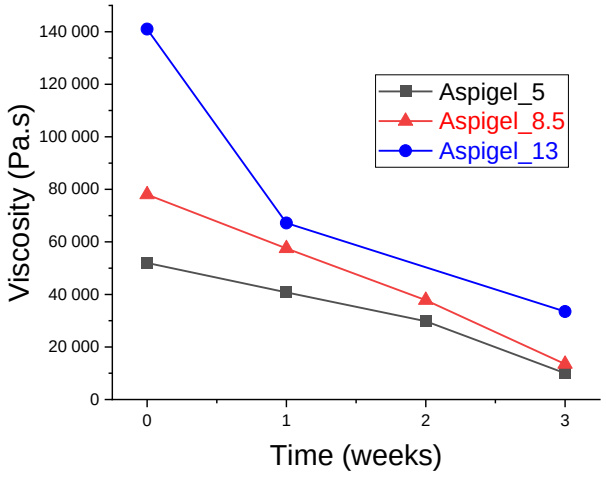


*Figure 42. Evolution with time of the viscosity plateau values, obtained at a shear rate of 0.015 $s^{-1}$, for the Aspigel_5 (black squares), Aspigel_8.5 (red triangles) and Aspigel_13 (blue circles).*

The aging of the gels induces a significant drop of their viscosities. Indeed, as shown above, $Fe_3O_4$ particles react and dissolve with the decontamination solution of the Aspigel 100E. This leads to a diminution of the solid concentration in the gel, which has strong influence on the gels viscosity [15]. Lower the amount of particles in the gel is, lower is the viscosity of the gel.

- Influence of the aging on the spreading and decontamination properties

The spreading as well as the decontamination of the Aspigel_5 and Aspigel _8.5 were evaluated at different storage times (Figure 43). Note that experiments were performed only on these two gels because Aspigel_8.5 and Aspigel_13 present similar performances, but the latter producing a larger secondary waste volume due to its higher content in ferromagnetic particles.

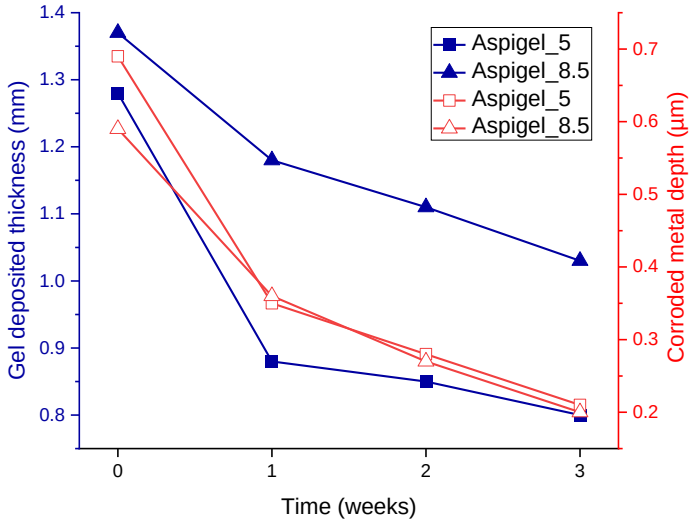


*Figure 43. Influence of the aging of the Aspigel_5 (square symbols) and the Aspigel_8.5 (triangle symbols) on their deposited thicknesses (blue full symbols) and their corrosion efficiency (red empty symbols).*

For the two gels, the gel deposited thickness decreases with the storage time, meaning their spreading properties are improved. This is in accordance with the drop of the viscosity. Even if some $Fe_3O_4$ particles are dissolved and may induce a loss of a part of the magnetic response of the gels, the drop of the viscosity has a stronger impact on the gel spreading properties. Moreover, the evolution of the spreading properties are more marked after one week of aging. Indeed, as observed on Figure 40, the dissolution rate of the $Fe_3O_4$ particles is higher during the first days.

The lower gel thicknesses have a direct influence on the corrosion depth of the SS coupons. For the first experiment performed at t = 0, the gel thickness is slightly larger for the Aspigel_8.5 than for the Aspigel_5, while this is the opposite for the SS corrosion depth. These differences are quite tenuous but can be explained by the chemical reaction between the $Fe_3O_4$ particles and the decontamination solution. Indeed, as the gel was evaluated one day rest after their formulation (see above), the Aspigel_8.5 may have consumed more decontamination reagents than the Aspigel_5. This is confirmed by the evolution with time. As the gel deposited layers are thinner for Aspigel_5, the metal corrosion depth remain similar between the two gels. Consequently, the presence of more particles decreases more significantly the efficiency of the decontamination solution. However, for both gels and storage time longer than 1 week, the attack of the SS is less than 0.3 µm. This will limit the application of such gels, depending on the thickness of the oxidized layer to remove.

### 3.2.4 Conclusion and perspectives

A new gel decontamination process was developed specifically for the decontamination of hardly accessible surfaces, such as the internal surface of pipes for example. This process is based on the modification of vacuumable gels by adding ferromagnetic particles in their formulations. Thus, the gels can be moved and spread using a magnet, placed more and less close to the gel, depending on the gel formulation and the magnet. After drying, the gel forms solid residues, which can also be recovered by the magnet. In this way, the all decontamination process is not necessarily implemented at the contact of the contaminated surface, and decontamination gels can be applied on hardly accessible surfaces.

It was demonstrated that the presence of ferromagnetic particles does not influence the inherently decontamination properties of a commercial gel, with similar corrosion efficiency and effect on the microstructure of the SS after treatment. However, the decontamination efficiency depends on the spreading of the gel and more particularly on the gel thickness. Notably, adding more particles increases the gel viscosity but does not particularly improve their spreading properties. Indeed, while ferromagnetic particles provide a magnetic response to the gel, adding more particles also increases the gel viscosity. That is why, a compromised has to be found between the ferromagnetic particles amount in the gel.

However, $Fe_3O_4$ particles react with the chemical solution of the Aspigel 100E and dissolve with time, inducing variation in the gel rheological properties. Consequently, spreading properties as well as the gel decontamination efficiency evolve with time, which is not compatible for a long time storage of the product, and it is recommended to formulate the gel just before application.

The efficiency of the “magnetic gel” process is directly related to the spreading properties of the gel. Thus, to better control the gel application, two main perspectives have been identified. First, the physicochemical properties of the ferromagnetic particles could be studied. Indeed, other natures of particles may present higher magnetic responses, allowing to both better spread the gel and limit the amount of generated secondary waste. Moreover, the influence of the type of magnet was not considered in this work. However, we may reasonably assume that the spreading of a gel formulation is also depending on the geometry and the power of the magnet. This point could be studied in the future.

# 4 Conclusions and perspectives

The decontamination of oxidized metallic surfaces needs the chemical dissolution of oxide layers to segregate the contaminated surface material from the bulk substrate. Among the different existing techniques, the vacuumable gels are interesting because they produced only secondary solid waste and limit the close contact of the operator with the contaminated surface. However, this technology currently also presents some limitations. This document reports the different studies performed during the PREDIS project with the objective to respond to these limitations.

First, we have shown that actual existing gels is not very efficient to eliminate multi-layered and strong corrosion layers of a few microns from a SS surface. In this way, new gel formulations, based on the COREMIX process, were developed. Particularly, two gels with satisfying rheological properties were formulated by using silica NPs as the viscosity agent: one containing 15 mmol.$L^{-1}$ of $KMnO_4$ and 3 mmol.$L^{-1}$ of $HNO_3$ able to oxidized a Cr-enriched oxide layer, and a second one containing 18.5 mmol.$L^{-1}$ of oxalic acid to dissolve the Fe oxide layer. These gels are intended to be used sequentially and proved to be efficient on slightly and moderated oxidized SS coupons. The process decontamination efficiency was compared with a commercial gel. Despite the commercial gel still has better performances than these new gels, these new COREMIX -based gels may present an interesting alternative. Indeed, as the commercial gel contains Ce(IV), the COREMIX-based gels could be used in situation where the presence of Ce(IV) is problematic or if the decontamination operation has to be very slight to not corrode deeply the surface. Moreover, the different gels evaluated in this work still have a low efficiency on strongly oxidized samples. This may be a limitation of the “vacuumable gel” process. The volume of decontamination solution at the contact of the substrate is proportional to the gel thickness and is consequently very low compared to a liquid bath for example. Then, during the evaporation step, the chemical reaction with the oxidized substrate is progressively hindered. That is why, even if the vacuumable gel process presents clear advantages in term secondary waste management, its efficiency seems to be restricted due to its intrinsic principle itself. As perspectives, further studies could be pursued but rather on the application process than on the development of new formulations. In particular, multiplying successive applications could induce several thin layer eliminations until the complete removal of the thick oxide layer. Shortening the drying time may also increase the contact time between the oxidized coupon and the decontamination solution for a longer chemical reaction. Experiments at higher temperatures could also be explored as a method to increase the reaction kinetic and improve the process efficiency.

The second limitation lies in the gel implementation mode by spraying or manual deposition. This mode is very well adapted to large and plane surfaces, but make the gel application difficult, even sometimes impossible, on items having complex geometries or hardly accessible surfaces (internal surface of pipes for example). Thus, two alternative implementation processes were studied. First, it was shown that existing commercial gels can be used as a bath in a dipping process. This allows the coating of small items with a homogenous gel layer and their decontamination.

Another innovative process, named “magnetic gel” process, was developed and patented during the PREDIS project. The addition of ferromagnetic particles in the formulation of gels provide them magnetic features, making them spreadable using a magnet. The magnet can be used more or less close to the gel, and even at the opposite phase of the contaminated surface. In this way, the gel can applied on hardly accessible surfaces. Moreover, after decontamination and drying, the secondary solid residues can be recovered also with a magnet.

This work has demonstrated the efficiency and the interest of the process as well as the existing relationship between the amount of ferromagnetic particles and their influence on the rheological and spreading properties of the gel. Thus, a small amount of ferromagnetic particles can be sufficient to spread the gel and present satisfying decontamination properties. However, due to the reaction between the ferromagnetic particles and the decontamination solution, the evolution of the gel formulation with time has to be taken into account because it has a strong influence on the gel spreading and chemical efficiency. From now, this process could be optimized for a better control of the gel spreading and it evolution with time.

For that, the study of the nature and physicochemical properties of the ferromagnetic particles is an interesting step to increase the gel magnetic response and limit the amount of generated secondary waste. Moreover, the type of magnet was not considered in this work. However, we may reasonably assume that it has a strong influence on the gel spreading and that there is a relationship between a gel formulation of the power and geometry of the magnet.

Finally, after these different studies, it is of interest to compare the results with other decontamination techniques. Criteria such as the decontamination efficiency, the nature and volume of generated secondary waste, but also the application possibilities of the processes should be evaluated to identify the strong and weak points of the different techniques, depending on the decontamination operation context. This work will be presented in the Deliverable 4.4 of the PREDIS project.

# REFERENCES

[1] Rivonkar, A., Katona, R., Robin, M., Suzuki-Muresan, T., Abdelouas, A., Mokili, M. Bator, G. & Kovacs, T. 2022. Optimisation of the chemical oxidation-reduction process (CORD) on surrogate stainless steel in regards to its efficiency and secondary wastes. Frontiers in Nuclear Engineering (1) 1080954.

[2] Barton, D.N.T., Grebennikova, T., Denman, A.E., Carey, T., Engelberg, D.L. & Sharrad, C.A. 2023. Long-term aqueous contamination of stainless steel in simulant nuclear reprocessing environments. Journal of Nuclear Materials (583) 154551.

[3] Zhong, L., Lei, J.H., Deng, J., Lei, Z., Lei, L. & Xu, X.S. 2021. Existing and potential decontamination methods for radioactively contaminated metals-A Review. Progess in Nuclear Energy (139) 103854.

[4] Gossard, A., Lilin, A. & Faure, S. 2022. Gels, coatings and foams for radioactive surface decontamination: State of the art and challenges for the nuclear industry. Progress in Nuclear Energy (149) 104255.

[5] Gossard, A., Frances, F. & Turc, H.A. 2022. Method for treating surfaces or gaseous media using a ferromagnetic gel. Patent WO2022/184996.

[6] Li, D., Lin, C., Batchelor-McAuley, C., Chen, L. & Compton R.G. 2018. Tafel analysis in practice. Journal of Electroanalytical Chemistry (826) 117-124.

[7] Castellani, R., Poulesquen, A., Goettmann, F., Marchal, P. & Choplin L. 2013. Ions effects on sol–gel transition and rheological behavior in alumina slurries. Colloids and Surfaces A: Physicochemical and Engineering Aspects (430) 39-45.

[8] Chen, S., Øye G. & Sjöblom, J. 2007. Effect of pH and Salt on Rheological Properties of Aerosil Suspensions. Journal of Dispersion Science and Technology (28) 845–53.

[9] Carey, T. & Callow, A. In preparation.

[10] Castellani, R., Poulesquen, A., Goettmann, F., Marchal, P. & Choplin, L. 2014. A topping gel for the treatment of nuclear contaminated small items. Nuclear Engineering and Design (278) 481-490.

[11] Gossard, A., Frances, F., Aloin, C., Penavayre, C., Fabrègue, N. & Lepeytre, C. 2021. Effect of Surfactant Concentration on the Long-Term Properties of a Colloidal Chemical, Biological and Radiological (CBR) Decontamination Gel. Fluids (6) 410.

[12] Faure, S., Fuentes, P. & Lallot, Y. 2007. Vacuumable gel for decontaminating surfaces and use thereof. Patent WO2007/039598.

[13] Gossard, A. & Lepeytre, C. 2017. An innovative green process for the depollution of Cr(VI)-contaminated surfaces using $TiO_2$-based photocatalytic gels. Journal of Environmental Chemical Engineering (5) 5573-5580.

[14] Gossard, A., Frances, F. & Aloin, C. 2017. Rheological properties of $TiO_2$ suspensions varied by shifting the electrostatic inter-particle interactions with an organic co-solvent. Colloids and Surfaces A: Physicochemical and Engineering Aspects (522) 425-432.

[15] Zhou, Z., Scales, P.J. & Boger, D.V. 2001. Chemical and physical control of the rheology of concentrated metal oxide suspensions. Chemical Engineering Science (56) 2901-2920.

[16] Cheng, T.L., Wen, Y.H. & Hawk, J.A. 2014. Diffuse-Interface Modeling and Multiscale-Relay Simulation of Metal Oxidation Kinetics—With Revisit on Wagner's Theory. The Journal of Physical Chemistry C (118) 1269–1284.

[17] Wang, K., Spatschek, R. 2023. Phase Field Study of Cr-Oxide Growth Kinetics in the Crofer 22 APU Alloy Supported by Wagner's Theory. Energies (16) 3574.